Electrical Power and Energy Systems 116 (2020) 105530

Contents lists available at ScienceDirect

Electrical Power and Energy Systems

journal homepage: www.elsevier.com/locate/ijepes

Dynamic incorporation of nonlinearity into MILP formulation for short-term hydro scheduling

Hans Ivar Skjelbred[a], Jiehong Kong[a,*], Olav Bjarte Fosso[b]

[a] Department of Energy Systems, SINTEF Energy Research, 7034 Trondheim, Norway
[b] Department of Electric Power Engineering, Norwegian University of Science and Technology, 7491 Trondheim, Norway

ARTICLE INFO

Keywords:
Hydropower production function
Hydro unit commitment
Piecewise linear approximation
Mixed integer linear programming
Short-term hydro scheduling

ABSTRACT

Optimization tools are widely used for solving the short-term hydro scheduling (STHS) problem in a cascaded hydro system. In a mixed integer linear programming (MILP)-based formulation, the nonlinear and non-convex hydropower production function (HPF) is represented by piecewise linear approximation. However, instead of using a set of predefined curves with static breakpoints or a preprocessing phase to define the complete relationship between the power output, the net head, and the water discharge, this paper proposes a novel method in which the breakpoints in the linearization are determined dynamically, taking into account the time-varying head effect, intake loss, penstock loss, tailrace loss, and head-dependent turbine efficiency. Only one binary variable is needed to indicate the on/off status and power generation of a unit per period. Furthermore, there are few studies available on how to represent the HPF precisely for the hydraulic system where penstocks are shared by multiple generating units. In this paper, we investigate three heuristics to explicitly incorporate the nonlinear and state-dependent power loss in shared penstocks into the STHS problem. The method and heuristics have been implemented in an operational STHS tool used by many hydropower producers in Nordic countries. We use a simple hydro system to illustrate the method and heuristics and a real hydro system in Northern Norway to study calculation efficiency and solution quality. The numerical results indicate that the proposed method can precisely represent the head-dependent and nonlinear operating characteristics of the generating units. The accurate modeling of a system with multi-level shared penstock configurations is crucial for obtaining the optimal unit commitment. The heuristics can effectively handle the power loss in shared penstock in various operating conditions.

The main notations used in the basic mathematical formulation of the short-term hydro scheduling (STHS) problem are listed above. The notations of the auxiliary sets, parameters and variables that help to define the breakpoints of the unit input/output (I/O) curve and present the heuristics for dealing with power loss in shared penstocks will be introduced in Sections 4 and 5, respectively.

Note that the hydraulic objects in the cascaded watercourse can be connected in both series and in parallel. A reservoir can be associated with a plant or be interconnected by a junction/gate. Therefore, we separate the sets and indexes of reservoirs and plants. If not specially mentioned, reservoir k always refers to the direct upstream reservoir of plant s and reservoir $k + 1$ refers to the direct downstream reservoir of plant s.

In addition, the asterisk "*" as superscript is added to the variable to indicate that it is the optimal result in the previous iteration and is used as the reference point in the current iteration. For example, $v^*_{k,t-1}$ refers to the water volume at the beginning of period t obtained after optimization in the previous iteration and will be employed to update the gross head at period t in the current iteration.

1. Introduction

Early practice in short-term hydro scheduling (STHS) was to optimally determine the water release of cascaded reservoirs and to attain power generation schedule of the available hydro resources during a time horizon from a single day to one week. Nowadays, the application of STHS to the power system integrated with non-dispatchable renewable energy brings about new business opportunities and scheduling challenges. Participation in both energy and capacity markets

Abbreviations: A, instance based on test example A; B, instance based on test example B; G, generator; H, heuristic; HPF, hydropower production function; I/O, input/output; LP, linear programming; MILP, mixed integer linear programming; MINLP, mixed integer nonlinear programming; SHOP, short-term hydro optimization program; STHS, short-term hydro scheduling; UC, unit commitment; ULD, unit load dispatch

* Corresponding author.
E-mail address: jiehong.kong@sintef.no (J. Kong).

https://doi.org/10.1016/j.ijepes.2019.105530
Received 22 March 2019; Received in revised form 3 August 2019; Accepted 1 September 2019
Available online 26 September 2019

Nomenclature

Sets and indexes

T set of time periods, index $t \in T$.
K set of reservoirs, index $k \in K$.
U_k set of all direct upstream hydraulic objects for reservoir k, index $u \in U_k$.
S set of hydropower plants, index $s \in S$.
N_s set of penstocks in plant s, index $n \in N_s$.
I_s set of units in plant s, index $i \in I_s$.
$I_{n,s}$ set of units that connect to the same penstock n in plant s, index $i \in I_{n,s}$.

Parameters

$\bar{t}$ number of the periods of the scheduling problem.
ΔT length of each period (hour, h).
$\tau_{u,k}$ water delay time from upstream hydraulic object u to reservoir k (h).
$V_{k,0}^{INIT}$ initial water storage of reservoir k (cubic meter, m^3).
V_k^{MIN}, V_k^{MAX} minimum and maximum water volume of reservoir k (m^3).
$Q_{k,t}^{NI}$ forecasted natural inflow into reservoir k in period t (cubic meter per second, m^3/s).
E_s energy conversion factor for plant s (megawatt-hour per cubic meter, MWh/m^3).
L_s water level at the outlet of plant s (m).
$\alpha_{n,s}$ loss factor of penstock n in plant s, taking into account the length, diameter, curvature, and roughness of the penstock's inner walls (s^2/m^5).
G conversion constant including the gravity acceleration and water density, default setting is $9.81 \bullet 10^{-3}$ ($kg \bullet m^2/s^2$).
$P_{i,s}^{MIN}$, $P_{i,s}^{MAX}$ minimum and maximum production of unit i in plant s (MW).
$\Omega_{i,s,0}$ initial status of unit i in plant s (1 on, 0 off).
$C_{i,s}$ start-up cost of unit i in plant s (€).
M_t^{SELL} forecasted market price of energy in period t (€/MWh).
$W_{k,\bar{t}}^{END}$ marginal water value of reservoir k at the end of the scheduling horizon $\bar{t}$ (€/MWh).

Variables

$\omega_{i,s,t} \in \{0, 1\}$ status of unit i in plant s in period t (1 on, 0 off).
$\mu_{i,s,t} \in \{0, 1\}$ start-up decision of unit i in plant s in period t (1 if it is started up in period t, 0 otherwise).
$v_{k,t}$ water volume of reservoir k at the end of period t (m^3).
$q_{k,t}^{TOTAL}$ total regulated water release of reservoir k in period t (m^3/s).
$h_{s,t}^{GROSS}$ gross head of plant s in period t (m).
$h_{i,s,t}^{NET}$ net head of unit i in plant s in period t (m).
$q_{i,s,t}$ water discharge of unit i in plant s in period t (m^3/s).
$p_{i,s,t}$ power output of unit i in plant s in period t (MW).
p_t^{SELL} power sold to the market in period t (MW).

State-dependent functions

$l_{k,t-1}(v_{k,t-1})$ water level of reservoir k as a function of the water volume of the reservoir (m).
$\Delta h_{s,t}^{INTAKE}(l_{k,t-1}, q_{k,t}^{TOTAL})$ intake head loss of plant s as a function of the water level of upstream reservoir k and the total regulated water release of the reservoir (m).
$\Delta h_{s,t}^{TAIL}(l_{k+1,t-1}, q_{k,t}^{TOTAL})$ tailrace head loss of plant s as a function of the water level of downstream reservoir $k+1$ and the total regulated water release of upstream reservoir k (m).
$\eta_{i,s}^{GEN}(p_{i,s,t})$ generator efficiency of unit i in plant s as a function of the production of the unit (%).
$\eta_{i,s}^{TURB}(h_{i,s,t}^{NET}, q_{i,s,t})$ turbine efficiency of unit i in plant s as a function of the net head and water discharge of the unit (%).
$Q_{i,s,t}^{MIN}(h_{i,s,t}^{NET})$, $Q_{i,s,t}^{MAX}(h_{i,s,t}^{NET})$ minimum and maximum water discharge of unit i in plant s in period t as a function of the net head (m^3/s).

highlights the need for precise calculation for energy conversion and available capacity of each unit.

The electric power produced by one generating unit is generally a nonlinear and non-convex function of the water discharge, the net head, and the turbine efficiency. The net head is defined as the difference between the gross head and the flow-related head losses due to the velocity of water flow (intake/tailrace loss) or the friction of water (penstock loss). The turbine efficiency is also a nonlinear function of the net head and the water discharge.

One of the conventional techniques to incorporate the nonlinearity of the hydropower production function (HPF) is to use a piecewise linear approximation. Together with the discrete nature such as the on/off status of the units or operational forbidden zones, the STHS problem is formulated as a mixed integer linear programming (MILP) model.

In the earlier work [1], the non-convex part in the low power operating region is omitted, and the HPF is approximated by a two-segment piecewise linear I/O curve, with breakpoints at best efficiency point and maximal discharge limit. In [2], binary variables are introduced to indicate the unit on/off generating status, and hence the first point of the two-segment linear curve starts from the minimum discharge limit. The head variation effect is first successfully modeled in [3] by developing a piecewise linear approximation of the nonlinear and non-convex I/O surface of water discharge and reservoir volume. The entire non-concave curves and head effect are considered through the use of binary variables. In [4], the authors proposed a tight representation of the head effect in which the linearization is enhanced through two-dimensional considerations of both water storages and flow. Instead of including all the candidate I/O curves in the formulation, an iterative procedure is introduced in [5] to successively update the head until convergence is achieved.

In [6], the authors discussed the effects of piecewise linearization of the nonlinear functions and presented a method to ensure the solution feasibility for the original nonlinear formulation of the HPF. In [7], based on the discretized net head intervals, the HPF is approximated as a set of piecewise curves and the head-sensitive characteristic of multiple irregularly shaped forbidden zones is effectively handled by several simple polygons.

MILP has been widely applied to solve large-scale STHS problems in the real world [8]. For example, authors in [9] used a case study of the Three Gorges Project, the world's largest and most complex hydropower system, with 32 heterogeneous generating units in operation, to demonstrate the accurate representation of the HPF by a three-dimensional piecewise linear approximation.

Though piecewise linear approximation of the HPF is a rather mature method with a rich body of literature, there is still room for improvement regarding solution accuracy and computational efficiency. In the literature, it is usually presumed that the breakpoints (i.e., the given pairs of water discharge and power output) of linear segments are specified in advance and are represented by a two-dimensional table for fixed-head (i.e., a single I/O curve [1,2]) or a three-dimensional matrix for head-sensitive (i.e., a family of I/O curves [3–7,9]). The actual power production values are calculated by an appropriate interpolation technique.

However, there are two challenges derived from this assumption: (1) How can we get the breakpoints *a priori*? A standard segmented regression with continuity and convexity constraints can be fitted to

historical operations data and determine the breakpoints. However, it is difficult to obtain sufficient historical data on the unit level [10]. In addition, the determination of all the breakpoints in the three-dimensional convex hull (i.e., the maximum production for a given grid with water discharge and reservoir volume) is time-consuming and requires a customized algorithm that takes into account the particular shape of the region to be calculated [11]. Dynamic programming in [12] and unit commitment (UC) heuristic algorithm in [13] are proposed to create a complete three-dimensional power output before optimization; (2) How can we solve the STHS problem within an acceptable time for daily operation? An accurate representation of the HPF is heavily dependent on the number of breakpoints and the net head intervals. Therefore, a large number of binary variables are used to represent the linear segments and the net head intervals, which will increase the solution time of the optimization problem. In order to avoid a large number of breakpoints, the authors presented a dynamic model where linear approximations are adjusted as the solving procedure of the problem evolves [14]. However, this method is based on the existence of a "complete" piecewise linear model with a very dense discretization grid (e.g., 1000 breakpoints in the flow axis).

On the other hand, in most STHS problems including the penstock head loss as a quadratic function of the turbined flow [6,7,13,15–21], there is a common premise that the penstock loss for one specific unit only depends on the water flow processed by that unit. It is correct only if the unit is fed by an independent penstock from the reservoir. However, in some areas, especially in the Norwegian hydro systems where most hydropower plants are built inside the mountains, multi-level shared penstock structures commonly exist for the sake of cost-saving. A hydropower plant consists of a main tunnel branching into several penstocks, through which the flowing water reaches multiple units [22]. For example, in Fig. 1, the flow of three units, G1-G3, all pass through the main tunnel of the plant. The flow of G1 only goes through Penstock1 while the flows of G2 and G3 both go through Penstock2. Therefore, the main tunnel and Penstock2 are shared penstocks (for clarity, we also call the main tunnel a penstock and use $\alpha_{0,s}$ to indicate the main tunnel that includes the parts from the reservoir to the dedicated penstocks and from the turbine to the discharge basin), whereas Penstock1 is an independent penstock.

The impact of the penstock loss cannot be ignored. It corresponds to the largest share of the total losses [23]. Even when the penstock loss only accounts for a tiny percentage of the gross head, ignoring it will directly influence the dispatch decision and result in inferior schedules [24]. Given the hydraulic system with shared penstocks, the calculation of penstock loss becomes considerably more complicated, involving not only the flow through the unit but also the flow of the other units connected to the same penstock [25]. Nevertheless, whether and at which level the units should run depend on how large the penstock loss is. This state-dependence makes it practically intractable to accurately model the penstock loss since the decisions of UC and unit load dispatch (ULD) are unknown prior to optimization.

How the loss in shared penstocks should be handled has not currently been explored to a great extent in the technical literature. Only a limited number of papers dealing with a single hydropower plant cover this subject. In [26], the authors used a tree structure to represent the multi-level configurations of the shared penstocks and proposed a decomposition algorithm to address the optimal distribution of the production among a set of online units. In [27], the ULD problem is solved by maximizing the end pressure of the shared penstock. A gauge pressure sensor is used to measure the flow at the end of the penstock. In [28], a two-phase decomposition approach is presented. The UC subproblem is solved by a hybrid algorithm that combines a heuristic searching method and a progressive optimal algorithm. Then the ULD subproblem is solved by dynamic programming.

Though it is widely admitted that a realistic and detailed representation of the HPF is critical in order to obtain reliable results, simplification cannot be avoided in most of the work reported in the literature. For example, the head keeps static without head variation or hydraulic losses [1]; the turbine efficiency is a fixed value [11,26,29] or only flow-dependent [12]; the penstock head loss is constant [9] or calculated as a percentage of the power output regardless of the flow going through the tunnel [11,29]; and the units are always connected to independent penstocks [6,7,13,15–21]. These types of simplification do not reflect the complexity of the real-world day-to-day operation and cannot match the requirements from hydropower producers.

In this paper, we deal with incorporating the nonlinearity of the HPF into the MILP formulation with the intention of removing the simplification employed in the existing literature. The method for determining the unit I/O curve and the heuristics for handling power loss in shared penstocks have been implemented in the Short-term Hydro Optimization Program (SHOP), an operational scheduling tool used by many large hydropower producers in Scandinavia as well as in Switzerland, Austria and Chile.

The main contributions of this paper are threefold: Firstly, instead of using a set of pre-specified I/O curves with static breakpoints or a preprocessing phase to define the complete relationship among the power output, the net head, and the water discharge, the breakpoints in the linearization are determined dynamically, taking into account the time-varying head effect, intake loss, penstock loss, tailrace loss, and head-dependent turbine efficiency. The basic idea of using an iterative procedure to refine the results was mentioned in [1,5,30]. However, no details about the applied modeling procedure were included. In this paper, a thorough mathematical formulation and a comprehensive process for determining the breakpoints of the I/O curve are provided.

Next, in contrast to the existing piecewise linear approximation of the HPF, in our proposed method the number of binary variables and constraints to model the state-dependent HPF is significantly reduced, and hence, the computational burden is diminished. Only one binary variable is needed to indicate the on/off status and power generation of a unit per period.

Finally, three heuristics are put forward to explicitly handle the nonlinear and state-dependent power loss in shared penstocks in the STHS problem. The first two heuristics, H1 and H2, directly include penstock loss in the determination of the breakpoints. The third heuristic, H3, first ignores the penstock loss when building the I/O curve of each unit, and then incorporates the loss in shared penstocks into the energy balance of the plant. By using a piecewise linear approximation, the nonlinear penstock loss can be effectively transformed into the framework of MILP.

In the case study, we use a simple hydro system to illustrate the method and heuristics and a real hydro system in Northern Norway to examine calculation efficiency and solution quality. The numerical results indicate that the proposed method can precisely represent the head-dependent and nonlinear operating characteristics of the generating units. The accurate modeling of a system with multi-level shared penstock configurations is crucial for obtaining the optimal UC. The heuristics can effectively handle the power loss in shared penstock in various operating conditions.

The remainder of this paper is as follows. In the next section, we

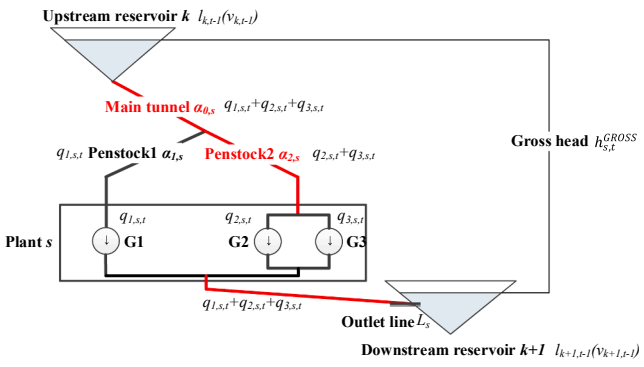

Fig. 1. Schematic diagram of the shared main tunnel and penstock.

formulate the basic mathematical model of the STHS problem. In Section 3, we summarize the solution methodology of SHOP, which is the foundation for choosing the appropriate modeling techniques to incorporate the nonlinearity of the HPF into the MILP formulation. In Section 4, the procedure for building the linear I/O curve based on the nonlinear HPF is given. Three heuristics for including power loss in shared penstocks in STHS are presented in Section 5. The determination of the unit I/O curve is illustrated, and the effectiveness of the heuristics are compared in Section 6. Concluding remarks and recommendations for further work are discussed in the last section.

2. Mathematical formulation of STHS

The goal of the STHS problem is to maximize the total profit subject to the hydrological balance of the reservoirs and power generation in the plants. In this section, the basic mixed integer nonlinear programming (MINLP) formulation is elaborated as follows.

2.1. Objective function

$$Max \sum_{t\in T} M_t^{SELL} \bullet \Delta T \bullet p_t^{SELL} + \sum_{k\in K} W_{k,\bar{t}}^{END} \bullet E_s \bullet v_{k,\bar{t}} - \sum_{t\in T}\sum_{s\in S}\sum_{i\in I_s} C_{i,s} \bullet \mu_{i,s,t} \tag{1}$$

The optimization problem is a trade-off between using the water now and saving it for future generation. Therefore, the total profit is the current revenue from selling energy in the market (first term in (1)) plus the future income by storing water at the end of scheduling horizon (second term) and minus the start-up cost of each unit (third term). Here, water value $W_{k,\bar{t}}^{END}$ is assumed to be a fixed value. It can also be expressed as a piecewise linear future cost function of the water volume in the reservoir. It is usually provided by a long-/mid-term hydro scheduling model that would integrate the stochastic nature of inflow, market price, load, and non-dispatchable renewable energy in the power system [31].

2.2. Water management in the reservoirs

$$v_{k,0} = V_{k,0}^{INIT}, \forall\, k \in K. \tag{2}$$

$$v_{k,t} = v_{k,t-1} + 3600 \bullet \Delta T \bullet \left(Q_{k,t}^{NI} + \sum_{u\in U_k} q_{u,t-\tau_{u,k}}^{TOTAL} - q_{k,t}^{TOTAL} \right), \forall\, k \in K, t \in T. \tag{3}$$

$$q_{k,t}^{TOTAL} = \sum_{i\in I_s} q_{i,s,t}, \forall\, k \in K, t \in T. \tag{4}$$

$$V_k^{MIN} \le v_{k,t} \le V_k^{MAX}, \forall\, k \in K, t \in T. \tag{5}$$

The hydrological balance of a cascaded reservoir k associated with plant s in each period is formulated in (2)–(4). These constraints are linearly coupled in time and space. The water storage of reservoir k at the end of period t is the storage at the beginning of the period $t-1$ plus the volume of inflow minus outflow in period t. The volume of flow is decided by the length of period ΔT (i.e., time resolution), and the constant "3600″ represents 3600 s in one hour. The total inflow includes the forecasted natural inflow and the water discharged from the upstream reservoirs or other hydraulic objects (e.g., gate, junction, and creek intake). Due to the cascaded hydraulic configuration, the fraction of water released upstream will contribute to the inflow of downstream reservoirs after a certain time delay. The outflow refers to the sum of the turbined flow to the downstream units. It could also include the regulated water release through the bypass gate and uncontrollable spillage over the reservoir. Eq. (5) restricts the allowable capacity of the reservoirs.

2.3. Head variation and flow-related head losses

$$h_{s,t}^{GROSS} = l_{k,t-1}(v_{k,t-1}) - \mathrm{MAX}[l_{k+1,t-1}(v_{k+1,t-1}), L_s], \forall\, s \in S, t \in T. \tag{6}$$

$$h_{i,s,t}^{NET} = h_{s,t}^{GROSS} - \sum_{n\in N_s | i\in I_{n,s}} \alpha_{n,s} \bullet \left(q_{i,s,t} + \sum_{i'\in I_{n,s}\setminus\{i\}} q_{i',s,t} \right)^2 - \Delta h_{s,t}^{INTAKE} (l_{k,t-1}(v_{k,t-1}), q_{k,t}^{TOTAL}) - \Delta h_{s,t}^{TAIL} (l_{k+1,t-1}(v_{k+1,t-1}), q_{k,t}^{TOTAL}), \forall\, i \in I_s, s \in S, t \in T. \tag{7}$$

The net head available at a turbine relies on the water level variation of the reservoirs (i.e., the gross head) and head losses. The gross head of the plant, expressed in (6), is the difference between the water level of the upstream reservoir, i.e., the forebay level, and downstream reservoir (if the water level of downstream reservoir $k+1$ is higher than the outlet line of the plant s). The water level can be formulated as a piecewise linear function of the water stored in the reservoir.

In addition, head losses lead to the reduction of the gross head, which in turn affects the power generated in the turbines. Head losses are cumulative along a path in the hydraulic network, depending on the flow in the different sections of the network from the upstream to the downstream water surfaces. There are three main types of flow-related head losses: (1) Penstock/main tunnel head loss (second term in (7)) is related to the friction of water on the penstock wall and can be represented as a quadratic function of the flow going through the penstock; (2) Canal intake head loss (third term) is associated with the water level of upstream reservoir and the water flow passing through the plant; (3) Tailrace elevation can vary considerably with an accumulation of the total water discharge of the plant. If a hydraulic cohesive relationship exists, the tailrace elevation is also influenced by the water level of the immediate downstream reservoir (fourth term). In this paper, both intake loss and tailrace loss are described by piecewise linear curves with discretized water level intervals of related reservoirs [32].

To sum up, the net head of a unit is a function of the flow of all the units in the plant. The coupling net head variable causes the modeling challenges concerning how to foretell the on/off status of other units, and furthermore, to quantify their water discharge when determining the I/O curve for the specific unit before optimization. The solution is based on the algorithm of SHOP presented in Section 3 and the three heuristics proposed in Section 5.

2.4. Hydropower production in the plants

$$p_{i,s,t} = G \bullet \eta_{i,s}^{GEN}(p_{i,s,t}) \bullet \eta_{i,s}^{TURB}(h_{i,s,t}^{NET}, q_{i,s,t}) \bullet h_{i,s,t}^{NET} \bullet q_{i,s,t}, \forall\, i \in I_s, s \in S, t \in T. \tag{8}$$

$$P_{i,s}^{MIN} \bullet \omega_{i,s,t} \le p_{i,s,t} \le P_{i,s}^{MAX} \bullet \omega_{i,s,t}, \forall\, i \in I_s, s \in S, t \in T. \tag{9}$$

$$Q_{i,s,t}^{MIN}(h_{i,s,t}^{NET}) \bullet \omega_{i,s,t} \le q_{i,s,t} \le Q_{i,s,t}^{MAX}(h_{i,s,t}^{NET}) \bullet \omega_{i,s,t}, \forall\, i \in I_s, s \in S, t \in T. \tag{10}$$

$$\omega_{i,s,0} = \Omega_{i,s,0}, \forall\, i \in I_s, s \in S. \tag{11}$$

$$\mu_{i,s,t} \ge \omega_{i,s,t} - \omega_{i,s,t-1}, \forall\, i \in I_s, s \in S, t \in T. \tag{12}$$

$$\sum_{s\in S}\sum_{i\in I_s} p_{i,s,t} = p_t^{SELL}, \forall\, t \in T. \tag{13}$$

For a generating unit, the power generated depends on the net head and the discharge rate of the water passing that unit. It also depends on the generator efficiency and the head-dependent turbine efficiency. Eq. (8) is the HPF that converts the kinetic energy of falling water (input) into electrical energy (output). Eq. (9) determines the minimum and maximum production limits of the generator, whereas (10) corresponds to the permissible discharge range of the turbine, which is also head-dependent. Eqs. (11) and (12) reflect the start-up decision of the unit,

based on the commitment status of the units during two consecutive periods. The electricity generated can be sold to the market. This relationship is represented by the energy balance constraint in (13).

As expressed in (8), the HPF is a complex nonlinear equation with the characteristic of state-dependency. The operating limits of the unit, (9) and (10), are complex, associated with the net head, turbine discharge, and generator output. If the net head is lower than the so-called nominal value, the turbine is unable to make the generator attain its maximum power output. Then the operating limit is decided by the variable maximum discharged outflow as a function of the net head $Q^{MAX}_{i,s,t}(h^{NET}_{i,s,t})$. On the other hand, if the net head is higher than the nominal value, the turbine could effectively reach a power level beyond the maximum output. Then the operating limit should be imposed by the power limit on the generator capabilities $P^{MAX}_{i,s}$. The minimum operating limit has the reverse behavior. In Section 4, we will discuss how to convert the nonlinear HPF into a linear I/O curve while considering the bounds restricted by (9) and (10).

3. Solution methodology of SHOP

SHOP is an STHS tool developed by SINTEF Energy Research and used by hydropower producers for daily operation. It considers complex watercourses with various strategic, physical, technical and market constraints [30].

The solution algorithm in SHOP is decomposed into two modes: UC mode and ULD mode, as illustrated in Fig. 2. Iterations are performed to stabilize the head variation in the reservoirs. The volume and water level of the reservoirs are updated after each iteration and used to calculate the gross head for the plants in the next iteration. In theory, the convergence measure can be chosen as (1) the highest mismatch of the water level for each period before and after update, (2) the maximum unbalance between the optimized power output from the optimization model and the recomputed power output based on the original nonlinear HPF, and (3) the relative change in the value of objective function between two consecutive iterations. If the value is smaller than a given tolerance, the iterative process finishes. This is a common approach to solving the state-dependency in the STHS problem [5,33–35]. In practice, due to the variety of physical configurations and operating conditions, the end-users of SHOP would like to decide the number of iterations according to their experience.

In the UC mode, a MILP model is solved to specify the on/off decision for each unit per period. The convergence criterion is typically met after three to five iterations, and an optimal UC plan is found. Then the ULD mode is activated. Binary variables are fixed to the result obtained in the last iteration in the UC mode. Only committed units will be included in the ULD mode. Then the model turns into pure linear programming (LP). A dispatch schedule regarding the exact generation level for each committed unit will be determined after two or three iterations.

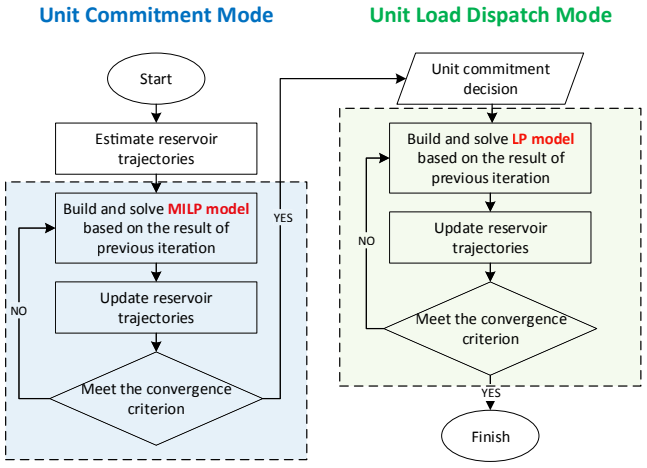

Fig. 2. Solution strategy of SHOP.

4. Method for determining the unit I/O curve

In this section, we will describe in detail the process of building the unit I/O curve based on the HPF. The main difference between the method proposed in this paper and those presented in the literature is that: (1) instead of representing the HPF as a family of I/O curves with given breakpoints [3–7,9], each breakpoint of the unit I/O curve is dynamically calculated for each period, considering the head variation, hydraulic losses, and head-dependent turbine efficiency; (2) rather than defining the complete unit discharge and generation relationship through a preprocessing phase and using a set of binary variables to validate the intervals of discharge and the head [12,13], only one I/O curve will be built and one binary variable is required to indicate the operating situation of the unit per period.

The notations used in this section are listed below:

X	Set of breakpoints/segments of the unit I/O curve, index $x \in X$.
$H^{GROSS}_{s,t}$	Gross head of the plant s in period t, subtracting the intake and tailrace head losses (m).
$Q^{BEST}_{i,s,t}(h^{NET}_{i,s,t})$	Best efficiency water discharge point of unit i in plant s in period t as a function of the net head (m^3/s).
$\overline{x}^{DOWN}$	The number of segments between the minimum water discharge $Q^{MIN}_{i,s,t}$ and the best efficiency $Q^{BEST}_{i,s,t}$.
$\overline{x}^{UP}$	The number of segments between the best efficiency $Q^{BEST}_{i,s,t}$ and the maximum water discharge $Q^{MAX}_{i,s,t}$.
$\overline{Q}_{x,i,s,t}$	Water discharge at breakpoint x of unit i in plant s in period t (m^3/s).
$\overline{P}_{x,i,s,t}$	Power output at breakpoint x of unit i in plant s in period t (MW).
$\overline{H}_{x,i,s,t}$	Net head at breakpoint x of unit i in plant s in period t (m).
$\gamma_{x,i,s,t}$	Slope of segment x of unit i in plant s in period t ($MW/m^3/s$).
$\hat{Q}^{MIN}_{i,s,t}$, $\hat{Q}^{MAX}_{i,s,t}$	Most restrictive minimum and maximum water discharge of unit i in plant s in period t (m^3/s).
$\hat{P}^{MIN}_{i,s,t}$, $\hat{P}^{MAX}_{i,s,t}$	Most restrictive minimum and maximum power output of unit i in plant s in period t (MW).
$q_{x,i,s,t}$	Water discharge of segment x of unit i in plant s in period t (m^3/s).

For period t, the process of building the I/O curve for unit i in plant s is summarized as follows. Fig. 3 illustrates the production and discharge at the breakpoints. The final unit I/O curve after convexification and the final operating limits determined by the most restrictive rule are highlighted in red.

Step 1: update the trajectory of the reservoir and calculate the gross head of the plant

As mentioned in the previous section, SHOP adopts an iterative procedure to update the trajectory of the reservoir. In the first iteration, the initial value of the reservoirs is used for the entire scheduling horizon. After solving the optimization problem, the volume $v^*_{k,t-1}$ and water level $l^*_{k,t-1}$ of the reservoirs for each period are updated, and therefore, the gross head of the plant can be determined.

If there exist intake loss and/or tailrace loss in a plant, we include them into the calculation of the gross head. After the first iteration, the optimal discharge of the units is obtained. Together with the updated water level of related reservoirs, intake and tailrace losses can be bilinearly interpolated, respectively.

In the next iteration, the gross head $H^{GROSS}_{s,t}$ is taken as a known parameter. Eq. (6) can thus be rewritten as follows:

$$H^{GROSS}_{s,t} = l^*_{k,t-1}(v^*_{k,t-1}) - \mathrm{MAX}[l^*_{k+1,t-1}(v^*_{k+1,t-1}), L_s] - \Delta h^{INTAKE}_{s,t}(l^*_{k,t-1}(v^*_{k,t-1}), q^{TOTAL*}_{k,t}) - \Delta h^{TAIL}_{s,t}(l^*_{k+1,t-1}(v^*_{k+1,t-1}), q^{TOTAL*}_{k,t}), \quad \forall s \in S, t \in T. \tag{14}$$

The net head at a working point of unit i becomes

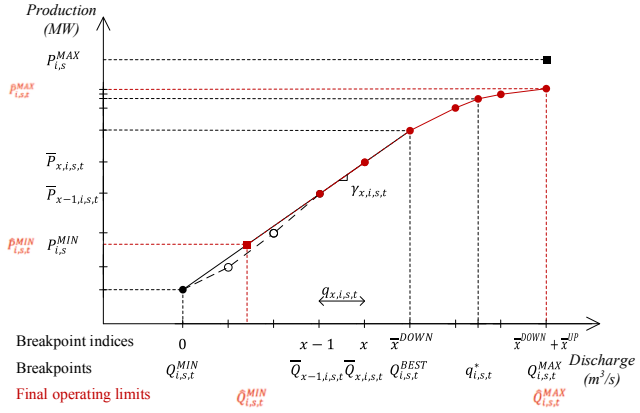

Fig. 3. Illustration for determining the concave piecewise linear unit I/O curve.

$$h_{i,s,t}^{NET} = H_{s,t}^{GROSS} - \sum_{n \in N_s | i \in I_{n,s}} \alpha_{n,s} \bullet \left(q_{i,s,t} + \sum_{i' \in I_{n,s} \setminus \{i\}} q_{i',s,t} \right)^2, \quad \forall\, i \in I_s,\ s \in S,\ t \in T. \tag{15}$$

Step 2: determine the head-dependent minimum water discharge $Q_{i,s,t}^{MIN}$, the best efficiency point $Q_{i,s,t}^{BEST}$ and the maximum water discharge $Q_{i,s,t}^{MAX}$ of the unit

The turbine efficiency is typically described by a Hill chart or Hill diagram, which is composed of a set of discrete triplets relating the turbine efficiency values, the net head, and the water discharge (Table 1). These points are usually provided by the turbine manufacturer [20] or in site measurement [36]. How to interpolate precise values from the Hill chart is beyond the scope of this paper. Interested readers can refer to [23,37]. Here we use bilinear interpolation to find the right efficiency for the given discharge and the net head.

Depending on the design and operating conditions of the turbine, the minimum, best efficiency, and maximum water discharge may keep constant or change with the net head. As an example, the minimum water discharge in Table 1 varies with the net head (30.45 m^3/s when the net head is 170 m, and decreases to 28.12 m^3/s when the head becomes 200 m, and then increases to 35.11 m^3/s when the head reaches 230 m), while the best efficiency point remains the same as 51.43 m^3/s for all the given net head levels.

If the minimum/best efficiency/maximum water discharge is constant, we can directly use the value without considering the effect of head variation. If the value varies with the net head, the net head must be first resolved. A simple iterative approach as illustrated in Fig. 4 can be used to stabilize the net head and to get the corresponding water discharge. Note that how to deal with the flow of other units fed by the same penstocks, i.e., $\sum_{i' \in I_{n,s} \setminus \{i\}} q_{i',s,t}$ in (15), will be discussed in Section 5.

Step 3: uniformly partition the interval between the minimum water discharge $Q_{i,s,t}^{MIN}$ and the best efficiency point $Q_{i,s,t}^{BEST}$ into $\bar{x}^{DOWN}$ segments

The discharges at the $\bar{x}^{DOWN} + 1$ breakpoints are denoted as in (16).

$$\overline{Q}_{x,i,s,t} = Q_{i,s,t}^{MIN} + \frac{Q_{i,s,t}^{BEST} - Q_{i,s,t}^{MIN}}{\bar{x}^{DOWN}} \bullet x, \quad \forall\, x = 0, \cdots, \bar{x}^{DOWN},\ i \in I_s,\ s \in S,\ t \in T. \tag{16}$$

Step 4: uniformly partition the interval between the best efficiency point $Q_{i,s,t}^{BEST}$ and the maximum water discharge $Q_{i,s,t}^{MAX}$ into $\bar{x}^{UP}$ segments

The discharge at the $\bar{x}^{UP}$ breakpoints are:

$$\overline{Q}_{x,i,s,t} = Q_{i,s,t}^{BEST} + \frac{Q_{i,s,t}^{MAX} - Q_{i,s,t}^{BEST}}{\bar{x}^{UP}} \bullet (x - \bar{x}^{DOWN}), \quad \forall\, x = x^{DOWN} + 1, \cdots, \bar{x}^{DOWN} + \bar{x}^{UP},\ i \in I_s,\ s \in S,\ t \in T. \tag{17}$$

Step 5: add the optimal operating point resulting from the previous iteration as an extra breakpoint

In the first iteration, *Steps 2–4* determine the discharge at each breakpoint of the unit I/O curve. After the first iteration, the optimal water discharge of the unit is decided. In the next iteration, if the optimal result from the previous iteration $q_{i,s,t}^{*}$ is different from any determined points in the I/O curve, it should be inserted as an extra breakpoint. This will improve the convergence since the breakpoints of the function are natural candidates to optimal solutions of the problem [14].

Step 6: calculate the corresponding power output at each breakpoint

Given a discharge point $\overline{Q}_{x,i,s,t}$ obtained from *Steps 2–5*, we can first use (15) to compute the net head $\overline{H}_{x,i,s,t}^{NET}$ and then apply bilinear interpolation to get the turbine efficiency $\eta_{i,s}^{TURB}(\overline{H}_{x,i,s,t}^{NET}, \overline{Q}_{x,i,s,t})$. The corresponding power output $\overline{P}_{x,i,s,t}$ can hence be calculated by (8). An iterative process initialized with the guess of generator efficiency $\eta_{i,s}^{GEN}$ is needed to stabilize the final output value [38].

Step 7: keep the slope of each segment Non-increasing by eliminating the nonconcave breakpoints

After the power output and the water discharge at all the breakpoints are established, the slope of each linear segment can be denoted as

$$\gamma_{x,i,s,t} = \frac{\overline{P}_{x,i,s,t} - \overline{P}_{x-1,i,s,t}}{\overline{Q}_{x,i,s,t} - \overline{Q}_{x-1,i,s,t}}, \quad \forall\, x \in X,\ i \in I_s,\ s \in S,\ t \in T. \tag{18}$$

As an operational scheduling tool primarily used for energy delivery and capacity allocation, SHOP should first be a computationally efficient deterministic model, and, then, can be used as a starting basis for incorporating stochastic features of the inflow and electricity prices [39], realizing the multi-purpose operations [40], and functioning in multi-market conditions [41]. To keep the computational burden as low as possible, a similar convexification as mentioned in [11] is employed to ensure the concavity of the I/O curve. The non-concave breakpoints (white points in Fig. 3) are removed, and the slope of the tandem linear segments must be non-increasing. The convexity of the optimization problem ensures that in the normal situation the flow variable of the upper segment $q_{x,i,s,t}$ is non-zero only when the flow variable of the

Table 1
Example of a Hill Curve table for turbine efficiency (%).

Discharge (m^3/s)	Efficiency (%)		
	Net head = 170 m	Net head = 200 m	Net head = 230 m
28.12	–	**86.73**	–
30.45	**87.03**	87.90	–
32.78	88.09	88.97	–
35.11	89.05	89.95	**90.84**
37.45	89.94	90.84	91.74
39.78	90.77	91.68	92.59
42.11	91.55	92.46	93.38
44.44	92.26	93.19	94.11
46.77	92.82	93.75	94.68
49.10	93.11	94.04	94.97
51.43	**93.22**	**94.15**	**95.08**
53.76	**93.04**	93.97	94.90
56.10	–	93.58	**94.51**
58.83	–	**93.10**	–

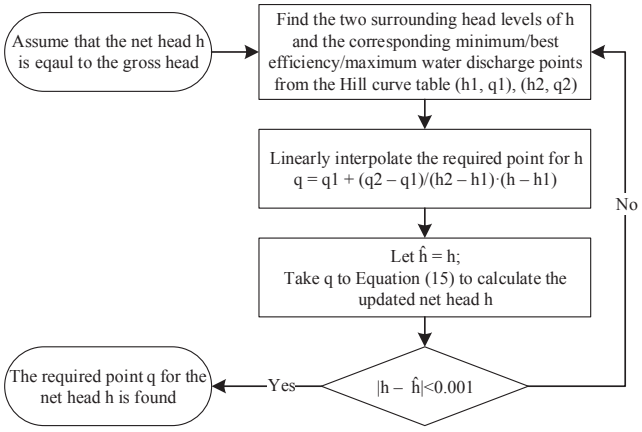

Fig. 4. The iterative approach to get the stable net head and the corresponding minimum/best efficiency/maximum water discharge.

lower segment $q_{x-1,i,s,t}$ fulfills its upper limit. As a result, instead of introducing binary variables for each linear segment, only one binary variable per unit is needed to indicate its running status.

Step 8: define the final operating limits based on the most restrictive rule

Now, the first and last breakpoints of the I/O curve are determined by the permissible discharge range of the turbine, i.e., (10). We should also include other limits, i.e., production bounds in (9). We hence define

$$\hat{P}_{i,s,t}^{MIN} = \text{MAX}[\overline{P}_{0,i,s,t}, P_{i,s}^{MIN}], \forall\, i \in I_s, s \in S, t \in T. \tag{19}$$

$$\hat{P}_{i,s,t}^{MAX} = \text{MIN}[\overline{P}_{\overline{x}^{DOWN}+\overline{x}^{UP},i,s,t}, P_{i,s}^{MAX}], \forall\, i \in I_s, s \in S, t \in T \tag{20}$$

The unit I/O curve in Fig. 3 may serve as an example. The minimum operating limit of the unit in period t is constrained by the minimum production of the generator, whereas the maximum operating limit is restricted by the maximum permissible water discharge of the turbine. The corresponding values of $\hat{Q}_{i,s,t}^{MIN}$, $\hat{Q}_{i,s,t}^{MAX}$ are linearly interpolated. The red line is the final piecewise linear I/O curve. Note that the operating limits and the chosen breakpoints in different periods vary with the change of the net head as well as the gross head.

Step 9: replace the HPF by a piecewise linear approximation

Finally, the HPF is represented by a piecewise linear I/O curve with the chosen breakpoints. In implementing the transformation, constraints (8)–(10) are replaced by the constraints (21)–(24).

$$p_{i,s,t} = \hat{P}_{i,s,t}^{MIN} \cdot \omega_{i,s,t} + \sum_{x \in X} \gamma_{x,i,s,t} \cdot q_{x,i,s,t}, \forall\, i \in I_s, s \in S, t \in T. \tag{21}$$

$$p_{i,s,t} \le \hat{P}_{i,s,t}^{MAX} \cdot \omega_{i,s,t}, \forall\, i \in I_s, s \in S, t \in T. \tag{22}$$

$$q_{i,s,t} = \hat{Q}_{i,s,t}^{MIN} \cdot \omega_{i,s,t} + \sum_{x \in X} q_{x,i,s,t}, \forall\, i \in I_s, s \in S, t \in T. \tag{23}$$

$$0 \le q_{x,i,s,t} \le \overline{Q}_{x,i,s,t} - \overline{Q}_{x-1,i,s,t}, \forall\, x \in X, i \in I_s, s \in S, t \in T. \tag{24}$$

5. Heuristics for incorporating power loss in shared penstocks into STHS

When using (15) to calculate the net head at one breakpoint, we notice that the net head relies not only on the current discharge rate of the unit but also on the operating status of other units that share the common penstocks. However, the determination of the unit I/O curve precedes the optimization. The operating status of other units remains unresolved. To resolve this challenge, we propose three different heuristics in this section.

The first heuristic H1 takes advantage of the solution strategy of SHOP. It uses the optimal discharge results obtained in the previous iteration to facilitate the calculation of the net head in the current iteration. The second heuristic H2 assumes that all the units connected to the same penstock always operate at the same proportion of their allowable capacity range. In the third heuristic, H3, the nonlinear power loss in shared penstocks is approximated by a convex piecewise linear function and incorporated into the MILP formulation.

One of the three heuristics must be selected in the UC mode to deal with the power loss in the shared penstocks. In the UC mode, the on/off decision of each unit will have an obvious impact on the calculation of power loss in the shared penstocks, and, in turn, the power loss has a direct influence on the determination of UC. In the ULD mode, the on/off status of all the units is already fixed. There are no significant changes in the production level of committed units between iterations. Then H1 is solely used to find the final schedules.

The notation used throughout this section is stated as follows:

Y	Set of breakpoints/segments of the power loss curve, index $y \in Y$.
$\overline{y}$	The number of segments of the power loss curve.
$\overline{Q}_{y,n,s,t}$	Water discharge at breakpoint y in penstock n in plant s in period t (m^3/s).
$\Delta\overline{P}_{y,n,s,t}$	Power loss at breakpoint y in penstock n in plant s in period t (MW).
$\gamma_{y,n,s,t}$	Slope of segment y in penstock n in plant s in period t (MW/m^3/s).
η	Turbine-generator efficiency (%).
$\Delta p_{i,s,t}$	Power loss of unit i in plant s in period t (MW).
$\Delta p_{n,s,t}$	Power loss in penstock n in plant s in period t (MW).
$q_{y,n,s,t}$	Water discharge of segment y in penstock n in plant s in period t (m^3/s).

5.1. H1

In H1, when calculating the net head at the breakpoints of the I/O curve of unit i, the optimal discharge results of other units i' from the previous iteration $q_{i',s,t}^{*}$ are taken as the current flow of those units. In the first iteration, we assume that the discharge of other units is 0. Then (15) becomes

$$\overline{H}_{x,i,s,t}^{NET} = H_{s,t}^{GROSS} - \sum_{n \in N_s | i \in I_{n,s}} \alpha_{n,s} \cdot \left(\overline{Q}_{x,i,s,t} + \sum_{i' \in I_{n,s} \setminus \{i\}} q_{i',s,t}^{*} \right)^2, \quad \forall\, x \in X, i \in I_s, s \in S, t \in T. \tag{25}$$

Under this setting, the power loss in the shared penstocks is directly included in the unit I/O curve. This heuristic will not cause any additional computational burden for the MILP problem in the UC mode. However, the main drawback of H1 is that convergence after iterations cannot be guaranteed in certain circumstances. The reason for this can be explained as follows. In the first iteration, the discharge of other units is assumed to be 0 when determining the net head at the breakpoints of the unit I/O curve. If other units are decided to run in the optimization, the net head is overestimated (i.e., underestimated power loss in shared penstocks). For a given discharge, the calculated production of the unit would be larger than the actual value. When the current electricity price is slightly higher than the future water value, it will just be profitable to produce the "high" output for the given discharge. Then the unit is committed to run. In the second iteration, the discharges of all the units are included in the calculation of the power loss. Then it will no longer be favorable to generate the "low" output for the same discharge. The unit is thus turned off. As a consequence, the UC decision oscillates between iterations.

5.2. H2

H2 is developed to avoid flip-flops in the UC decision. Instead of using the optimal results from the previous iteration, we assume that all the units fed by the shared penstocks run at the same proportion of the permissible discharge range. Given any discharge $\overline{Q}_{x,i,s,t}$ at the breakpoint for unit i, the corresponding discharge of other units $\overline{Q}_{x,i',s,t}$ is expressed as

$$\overline{Q}_{x,i',s,t} = Q^{MIN}_{i',s,t} + \frac{Q^{MAX}_{i',s,t} - Q^{MIN}_{i',s,t}}{Q^{MAX}_{i,s,t} - Q^{MIN}_{i,s,t}} \bullet (\overline{Q}_{x,i,s,t} - Q^{MIN}_{i,s,t}), \forall\, x \in X, \\ i' \in I_{n,s} \setminus \{i\}, n \in N_s|_{i \in I_{n,s}}, s \in S, t \in T. \tag{26}$$

Then the net head at that breakpoint is calculated as

$$\overline{H}^{NET}_{x,i,s,t} = H^{GROSS}_{s,t} - \sum_{n \in N_s|_{i \in I_{n,s}}} \alpha_{n,s} \bullet \left(\overline{Q}_{x,i,s,t} + \sum_{i' \in I_{n,s} \setminus \{i\}} \overline{Q}_{x,i',s,t} \right)^2, \\ \forall\, x \in X, i \in I_s, s \in S, t \in T. \tag{27}$$

Note that if the units are identical, H2 implies that all the units always operate at the same rate. An equitable power dispatch is an acceptable assumption in the existing literature [15,42]. However, even though the units are identical, with the same type of turbines and penstocks, there will be a difference in a unit dispatch because of the hydraulic losses. This difference will be even greater in those hydropower plants that possess multiple units with different operating characteristics [23]. Therefore, H2 may lead to an inferior solution.

5.3. H3

In contrast to H1 and H2 that directly include the head loss in shared penstocks in the determination of the unit I/O curve, H3 excludes the penstock head loss from the I/O curve. That is to say, the net head $h^{NET}_{i,s,t}$ is replaced with the gross head $H^{GROSS}_{s,t}$, and the power output at each breakpoint turns into

$$\overline{P}_{x,i,s,t} = G \bullet \eta^{GEN}_{i,s}(\overline{P}_{x,i,s,t}) \bullet \eta^{TURB}_{i,s}(H^{GROSS}_{s,t}, \overline{Q}_{x,i,s,t}) \bullet H^{GROSS}_{s,t} \bullet \overline{Q}_{x,i,s,t}, \\ \forall\, x \in X, i \in I_s, s \in S, t \in T. \tag{28}$$

In this way, the power production of the unit only depends on its own flow rate. However, the power output $p_{i,s,t}$ in (21) will thus be overestimated for the given water discharge $q_{i,s,t}$. To offset the excess, the sum of power loss in shared penstocks must be subtracted from the energy balance constraint.

The power loss of unit i can be defined as

$$\Delta p_{i,s,t} = G \bullet \eta \bullet \sum_{n \in N_s|_{i \in I_{n,s}}} \alpha_{n,s} \bullet \left(q_{i,s,t} + \sum_{i' \in I_{n,s} \setminus \{i\}} q_{i',s,t} \right)^2 \bullet q_{i,s,t}, \\ \forall\, i \in I_s, s \in S, t \in T. \tag{29}$$

To keep the formulation tractable, in the equations related to the power loss in the shared penstock it is assumed that the turbine-generator efficiency is a constant value η, rather than the product of $\eta^{GEN}_{i,s}(p_{i,s,t})$ and $\eta^{TURB}_{i,s}(h^{NET}_{i,s,t}, q_{i,s,t})$.

After adding together the power loss of all the units in the plant and reformulating the equation as (30), we find that the sum of power loss of each unit $\Delta p_{i,s,t}$ is equal to the sum of power loss in each penstock $\Delta p_{n,s,t}$, which is a cubic function of the total flow going through penstock n.

$$\sum_{i \in I_s} \Delta p_{i,s,t} = \sum_{n \in N_s} G \bullet \eta \bullet \alpha_{n,s} \bullet \left(\sum_{i \in I_{n,s}} q_{i,s,t} \right)^3 = \sum_{n \in N_s} \Delta p_{n,s,t}, \forall\, s \in S, t \in T. \tag{30}$$

We use the piecewise linear approximation to incorporate the nonlinear power loss function into the MILP formulation framework. The maximum flow that can pass through penstock n is the sum of maximum allowable water flow processed by each unit connecting to this penstock, i.e., $\sum_{i \in I_{n,s}} Q^{MAX}_{i,s,t}$. The interval $\left[0, \sum_{i \in I_{n,s}} Q^{MAX}_{i,s,t}\right]$ can be equally divided into $\bar{y}$ segments. The discharge and power loss at the breakpoints and the slope of linear segments are denoted as

$$\overline{Q}_{y,n,s,t} = \frac{\sum_{i \in I_{n,s}} Q^{MAX}_{i,s,t}}{\bar{y}} \bullet y, \forall\, y \in Y, n \in N_s, s \in S, t \in T. \tag{31}$$

$$\Delta \overline{P}_{y,n,s,t} = G \bullet \eta \bullet \alpha_{n,s} \bullet (\overline{Q}_{y,n,s,t})^3, \forall\, y \in Y, n \in N_s, s \in S, t \in T. \tag{32}$$

$$\gamma_{y,n,s,t} = \frac{\Delta \overline{P}_{y,n,s,t} - \Delta \overline{P}_{y-1,n,s,t}}{\overline{Q}_{y,n,s,t} - \overline{Q}_{y-1,n,s,t}}, \forall\, y \in Y, n \in N_s, s \in S, t \in T. \tag{33}$$

Then the power loss in the shared penstock is approximated by a convex piecewise linear function, as represented in (34).

$$\Delta p_{n,s,t} = \sum_{y \in Y} \gamma_{y,n,s,t} \bullet q_{y,n,s,t}, \forall\, n \in N_s, s \in S, t \in T. \tag{34}$$

$$0 \le q_{y,n,s,t} \le \frac{\sum_{i \in I_{n,s}} Q^{MAX}_{i,s,t}}{\bar{y}}, \forall\, y \in Y, n \in N_s, s \in S, t \in T. \tag{35}$$

$$\sum_{y \in Y} q_{y,n,s,t} = \sum_{i \in I_{n,s}} q_{i,s,t}, \forall\, n \in N_s, s \in S, t \in T. \tag{36}$$

Eq. (36) ensures that the water flow in the penstock should be the same as the sum of the flow of the units fed by the same penstock. In implementing H3, Eqs. (34)–(36) should be included in the final MILP formulation.

At last, we must subtract the power loss in all the shared penstocks from the energy balance constraint (13). Then (13) is modified as

$$\sum_{s \in S} \sum_{i \in I_s} p_{i,s,t} - \sum_{s \in S} \sum_{n \in N_s} \Delta p_{n,s,t} = p^{SELL}_t, \forall\, t \in T. \tag{37}$$

Table 2 summarizes the different MILP formulations in the UC mode by the three heuristics H1–H3 and in the ULD mode by H1.

6. Numerical results

In this section, we first use a simple hydro system to illustrate the method for determining the unit I/O curve and the three heuristics for handling the power loss in shared penstocks. Then we take a real Norwegian watercourse with cascaded reservoirs and plants to study calculational efficiency and solution quality with different heuristics and setting of parameters for both unit I/O curves and power loss curves.

All the instances are run by SHOP 12.10.0.a on an Intel Core i7-6600U processor with 16 GB of RAM. CPLEX 12.8.0 is the solver.

6.1. Test example A: a simple hydro system

The simple hydro system consists of one reservoir, one plant, and two identical units. Neither intake loss nor tailrace loss is considered. Furthermore, there is only one-level penstock structure, i.e., units are fed by a shared penstock or two independent penstocks directly from the upstream reservoir (Fig. 5). Loss factor for all the penstocks is 0.001. The reason why we choose such a basic topology is to avoid any disturbance and make the presentation concise to understand.

The piecewise linear relationship between reservoir volume and water level, together with the initial value, is described in Fig. 6. There is no inflow during the study period. The outlet line of the plant is 672 m. The minimum and maximum production limits of the unit are 60 MW and 120 MW. The unit start-up cost is set to 0 to eliminate its impact on the decision of UC. Then, the production will be affected purely by the relationship between the market price and the water value. Two types of turbine efficiency, with constant or variable

Table 2
= .

	UC Mode		ULD Mode
H1	H2	H3	H1
Objective function			
(1)	(1)	(1)	(1)[a]
Water management in the reservoirs			
(2)–(5)	(2)–(5)	(2)–(5)	(2)–(5)
On/off decision of the unit			
(11), (12)	(11), (12)	(11), (12)	–
Hydropower production function			
(21)–(24)	(21)–(24)	(21)–(24)	(21)–(24)[b]
Net head calculation when determining the unit I/O curve			
(25)	(27)	–	(25)
Linearization of power loss in shared penstocks			
–	–	(34)–(36)	–
Energy balance			
(13)	(13)	(37)	(13)

Note:
[a] $\mu_{i,s,t}$ in (1) are fixed to the result obtained in the last iteration in the UC mode.
[b] $\omega_{i,s,t}$ in (21) – (23) are fixed to the result obtained in the last iteration in the UC mode.

minimum/maximum discharge limits, are given in Figs. 7 and 8. Note that the curves in Fig. 8 matches the figures in Table 1. Generator efficiency is assumed to be 100% for the entire operating range.

Fig. 9 shows the market price profile of the day-ahead electricity market in Nord Pool from 0:00 23rd January to 0:00 26th January 2018 [43]. Two water value levels are used. The medium water value represents the marginal worth of stored water in the reservoir at the end of the 24-h scheduling horizon, while the low one indicates the value at the end of the 72-h scheduling horizon.

As cataloged in Table 3, we generate ten instances A1–A10 and perform four comparisons to analyze the impact of the three proposed heuristics, the modeling of penstock structure, the water value, and the unit operating limits on the STHS results. When determining the I/O curve per unit and period, the number of segments between the minimum water discharge and the best efficiency $\bar{x}^{DOWN}$ and the number of segments between the best efficiency and the maximum water discharge $\bar{x}^{UP}$ are both set to 3. When approximating power loss in shared penstock, the number of segments of the power loss curve $\bar{y}$ is 10.

Table 4 lists the relative profit changes between two consecutive iterations and the final objective function values for the instances. If not specifically mentioned, the "final" result for each instance refers to the solution obtained after five iterations in the UC mode and three iterations in the ULD mode. The detailed explanation for the figures will be given in the associated analysis of comparisons.

In the UC mode, the stopping criterion of each iteration is that the absolute MIP gap is 0. The computational time of each iteration, either in the UC mode or the ULD mode, is less than 0.05 s. The convergence measure is that the relative change in total profit between two consecutive iterations is less than 0.0005%. Except for A1 and A10, other instances all achieve convergence within the required iterations, in both UC and ULD modes.

6.1.1. Comparison 1: the impact of the three heuristics on the determination of the unit I/O curve

Comparison 1 is to demonstrate how the proposed heuristics influence the determination of the unit I/O curve, and furthermore, the production schedules. It is based on the hydro system where one shared penstock delivers water from the reservoir to the turbines (left graph in Fig. 5). The discharge limits of turbine efficiency are constant (Fig. 7). The water value is medium as 38 €/MWh, and the scheduling horizon is 24 h with hourly time resolution (blue dashed line in Fig. 9). Since the market price is lower than the water value in the first 6 h, no units are under operation during those periods. To indicate the changes in the I/O curve between iterations, unit G1 in Hour 7 when the plant starts to run is selected.

Fig. 10 depicts the I/O curves for G1 in Hour 7, established by heuristic H1, in the first and second iteration in the UC mode, respectively. Table 5 enumerates the determination of the final I/O curve in the first iteration. The breakpoints are defined according to the sequence as presented in Section 4. Consistent with *Step 2*, the I/O curve is originally constrained by the minimum and maximum operating limits of the turbine, i.e., 28.12 m^3/s and 58.83 m^3/s (See Fig. 7). As explained in *Step 7*, the second original breakpoint (35.99, 72.7) has to be eliminated when calculating the convex hull. Then all the tandem slopes become non-increasing. Concluded by *Step 8*, the final operating limits are defined by the most restrictive rule, i.e., the minimum and maximum production of the generator, 60 MW (the corresponding discharge 30.35 m^3/s is linearly interpolated) and 120 MW (57.92 m^3/s).

The optimal discharge rate for both units G1 and G2, after the first iteration, is 53.90 m^3/s. It is the same as one of the chosen breakpoints. Therefore, no extra point is added in the building of I/O curve in the second iteration (see *Step 5*). The discharge of G2 is assumed to be 0 in the first iteration, while the value becomes 53.90 m^3/s in the second iteration. Therefore, by H1, the production at each breakpoint in the second iteration (green dot in Fig. 10) is lower than those calculated in the first iteration (blue dot) for the same discharge. Note that given the same maximum point of the turbine (58.83 m^3/s), the production is reduced from 121.6 MW (in the first iteration) to 116.3 MW (in the second iteration). Then the final maximum operating limit is changed from the maximum production of the generator (120 MW) to the maximum discharge of the turbine (58.83 m^3/s). The reduction of production indicates that power loss in the shared penstock is considered in the determination of the unit I/O curve.

By contrast, there is no difference between iterations in the I/O curves built by heuristics H2 and H3 (Fig. 11). Instead of using the discharge result of G2 from the previous iteration as H1, H2 assumes both G1 and G2 run at the same fraction of the permissible discharge range. The production at each breakpoint is calculated by a stable combination of discharge points. On the other hand, by H3, the production at breakpoints is based on the gross head and power loss in the shared penstock is not included in the I/O curve. Therefore, given the same discharge, the power output by H3 (orange and yellow dots in Fig. 11) is higher than that obtained by H2 (black and gray dots).

Fig. 12 shows the evolution of the water level before each iteration by the three heuristics. As mentioned in *Step 1* in Section 4, in the first iteration, the initial water level (900 m) is used over the timespan. After the first iteration, the water level is updated by the optimal result and begins to reflect the changes in each period. It should be noted that the main difference in the results happens in Hours 13–17 when the water value is very close to the market price.

Just as discussed in Subsection 5.1, the oscillation of the UC decision in A1 results from the fact that, when the market price for selling

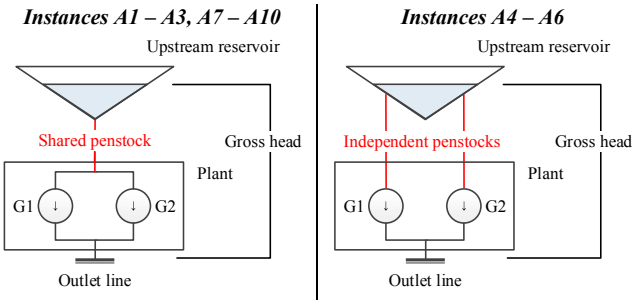

Fig. 5. Schematic diagram of the simple reservoir-plant topology.

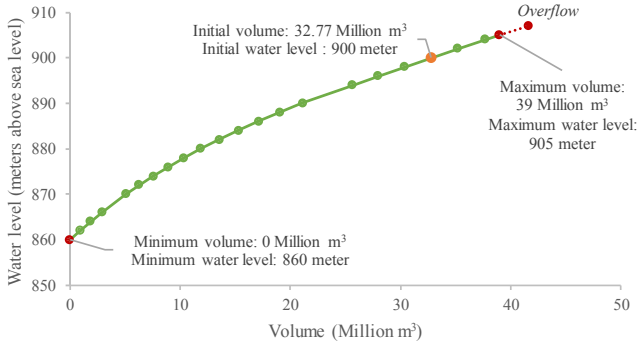

Fig. 6. Piecewise linear relationship between reservoir volume and water level.

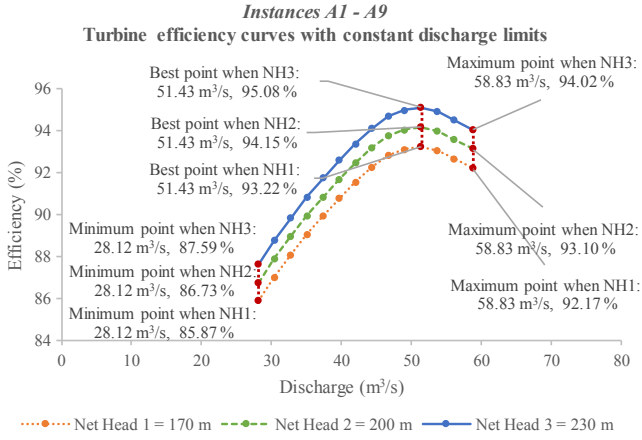

Fig. 7. Turbine efficiency curves with constant discharge limits.

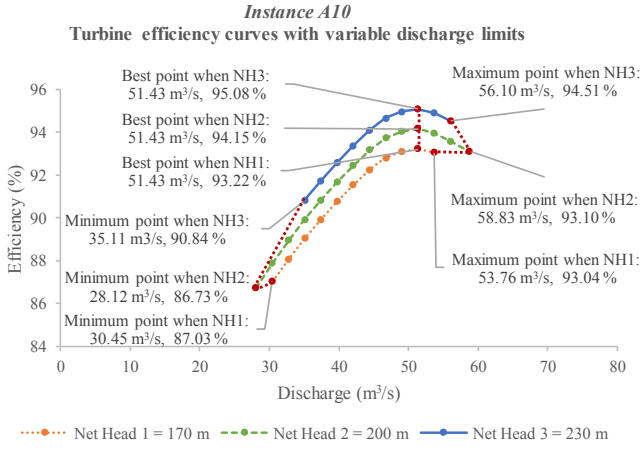

Fig. 8. Turbine efficiency curves with variable discharge limits.

energy is slightly higher than the water value of storing water, whether to produce depends on how significant the power loss is. In the first iteration, when the discharge of the other unit is not considered, the power loss in the shared penstock is lower than the actual value. The production is overrated, and both units are hence committed to run. In the second iteration, the discharge of the other unit is included in the calculation of penstock power loss. The increased power loss makes it no longer profitable to generate power. Then both units are turned off. Therefore, H1 fails to provide a stable UC decision when the market price and the water value are nearly the same. In other words, H1 cannot give reliable results in this situation.

In A2, H2 decides that both units run in Hour 14 and neither operates in Hours 15 and 16. In A3, H3 suggests that only G1 runs at best

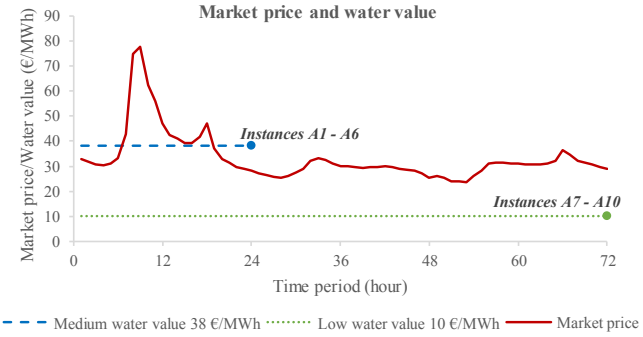

Fig. 9. Market price and two reservoir water values at the end of the two scheduling horizons.

Table 3
Information for Instances A1–A10 under Comparisons 1–4.

Instance	Heuristic	Penstock	Water value	Operating limits
Comparison 1: the impact of the three heuristics				
A1	H1	Shared	Medium	Constant
A2	H2	Shared	Medium	Constant
A3	H3	Shared	Medium	Constant
Comparison 2: the impact of modeling penstock structure				
A4	H1	Independent	Medium	Constant
A5	H2	Independent	Medium	Constant
A6	H3	Independent	Medium	Constant
Comparison 3: the impact of water value				
A7	H1	Shared	Low	Constant
A8	H2	Shared	Low	Constant
A9	H3	Shared	Low	Constant
Comparison 4: the impact of turbine efficiency curves				
A9	H3	Shared	Low	Constant
A10	H3	Shared	Low	Variable

efficiency while G2 stands still for these hours. As can be seen in Table 4, A3 solved by H3 yields higher profits than A2 run by H2.

6.1.2. Comparison 2: the impact of modeling penstock structure on the UC decision

Comparison 2 is to highlight the importance of modeling the penstock properly. Instances A1–A3 represent the actual situation that two units are connected to a shared penstock. Instances A4–A6 assumes that each unit is fed by an independent penstock (right graph in Fig. 5), which is the common assumption in most formulations of the STHS problem that accounts for the penstock loss.

As can be seen in Table 4, A4–A6 end up with the same results. The reason is that once the penstock is modeled as an independent channel, the power loss for unit G1 only depends on the water flow processed by G1. The operating status of G2 will no longer influence either the UC decision or the production level of G1. Therefore, no matter which heuristic is applied, there is no difference in the results.

To further understand the importance of the precise representation of the hydraulic system, the final water discharge of the units in A2 and A5 (run by heuristic H2), A3 and A6 (run by H3), is contrasted in Figs. 13 and 14, respectively. Note that since A1 solved by H1 fails to converge, there is no meaning to include A1 for comparison. The essential difference between these instances arises in Hours 14–16. If both units run at the same discharge rate, the sum of power loss in two independent penstocks (A5 and A6) will be smaller than the power loss in one shared penstock (A2 and A3). As already mentioned, the market price and the water value in Hours 14–16 are very close, the difference in power loss leads to a divergent UC decision. That is to say, more units are committed to run than necessary when the penstock structure is modeled as an independent.

If we apply the solution derived from A5 (or A6) as the production schedules into the actual situation with a shared penstock, the objective

Table 4
Results for Instances A1–A10.

	Instance A1[a]	A2	A3	A4	A5	A6	A7	A8	A9	A10[b]
Relative profit change between two consecutive iterations in the UC mode										
1st and 2nd iteration	−0.8879%	−0.1030%	0.0022%	−0.1339%	−0.1339%	−0.1339%	−10.069%	−6.5275%	−1.9523%	−2.1975%
2nd and 3rd iteration	0.0592%	0.0003%	−0.0014%	−0.0003%	−0.0003%	−0.0003%	−0.2541%	0.0000%	−0.9880%	−0.8371%
3rd and 4th iteration	−0.0464%	0.0000%	0.0000%	0.0000%	0.0000%	0.0000%	0.0000%	0.0000%	−0.0008%	−0.0191%
4th and 5th iteration	0.0465%	0.0000%	0.0000%	0.0000%	0.0000%	0.0000%	0.0000%	0.0000%	−0.0001%	−0.0002%
Relative profit change between two consecutive iterations in the ULD mode										
1st and 2nd iteration	0.0018%	0.0000%	0.0028%	0.0000%	0.0000%	0.0000%	0.0000%	0.0000%	0.6881%	1.2597%
2nd and 3rd iteration	0.0000%	0.0000%	0.0000%	0.0000%	0.0000%	0.0000%	0.0000%	0.0000%	0.0000%	−0.0456%
Final result										
Current revenue (€)	129,744	116,159	120,511	140,877	140,877	140,877	516,290	516,290	516,290	510,233
Future income (€)	625,302	639,230	635,088	620,140	620,140	620,140	13,249	13,249	13,249	16,367
Total profit (€)	755,046	755,389	755,599	761,017	761,017	761,017	529,539	529,539	529,539	526,600

Note:
[a] A1 incurs the flip-flop problem in the UC mode, and the iterations fail to converge. Therefore, the corresponding result is not acceptable.
[b] A10 achieves convergence in the ULD mode after five iterations. The final result is obtained after five iterations in both UC mode and ULD mode.

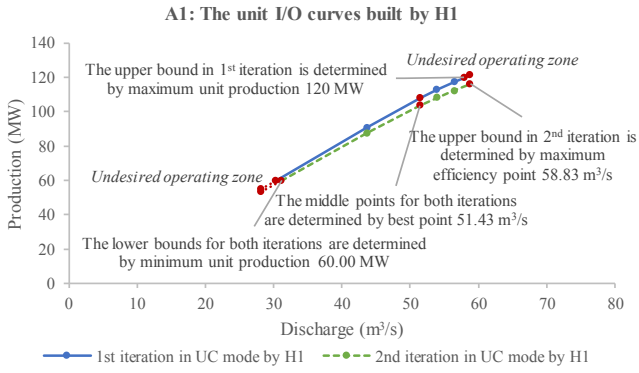

Fig. 10. The I/O curves for G1 in Hour 7 in the first and second iteration in the UC mode in A1.

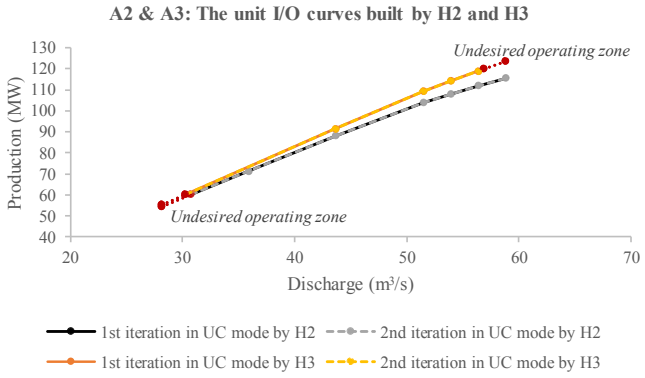

Fig. 11. The I/O curves for G1 in Hour 7 in the first and second iteration in the UC mode in A2 and A3.

function value becomes 754,639 €. In other words, the effect of disregarding the configuration of shared penstocks and modeling them as independent penstocks leads to the deviation from the optimal solution of −6,378 €. This effect will bring about an inferior solution in real-world operations.

6.1.3. Comparison 3: the impact of water value on the choice of the heuristics

Comparison 3 is to show that the relationship between the water value and the market price can make the STHS result more or less sensitive to the choice of heuristics. The water value in instances A7–A9 is as low as 10 €/MWh. The scheduling horizon becomes 72 h (green dotted line in Fig. 9).

In A1–A3, the water value is close to the market price during Hours 13–16, and hence, the result varies distinctly among the three heuristics. In A7–A9, the water value is so low that all heuristics find the same final optimal solution, though not at the first several iterations, to produce at maximum during the entire scheduling horizon (Table 4). Therefore, when there is an obvious discrepancy between the water value and the market price, other criteria such as calculational time are recommended for selecting the most suitable heuristic to solve the optimization problem. The variation in calculational time caused by different heuristics is shown in Table 7 under a real hydro system. The detailed explanation is given in *Comparison 5*.

6.1.4. Comparison 4: the impact of turbine efficiency curves on the operational limits of the units

Comparison 4 is to illustrate how the head-dependent discharge limits of the turbine and the running status of other units in the same plant influence the determination of I/O curves for the current unit. In this comparison, we run instances A9 and A10 by heuristic H3, respectively.

In both instances, the market price during the 72 h is significantly higher than the water value at the end of the scheduling horizon (green

Table 5
Determination of the I/O curve for G1 in Hour 7 in the first iteration in the UC mode in A1.

Original I/O curve			After convexification			Final I/O curve		
I (m^3/s)	O (MW)	Slope	I (m^3/s)	O (MW)	Slope	I (m^3/s)	O (MW)	Slope
28.12	54.8		28.12	54.8		30.35	**60.0**	
35.89	72.7	2.29	43.66	90.8	2.31	43.66	90.8	2.31
43.66	90.8	***2.33***	51.43	107.9	2.21	51.43	107.9	2.21
51.43	107.9	2.21	53.90	112.7	1.94	53.90	112.7	1.94
53.90	112.7	1.94	56.36	117.2	1.82	56.36	117.2	1.82
56.36	117.2	1.82	58.83	121.6	1.78	57.92	**120.0**	1.78
58.83	121.6	1.78						

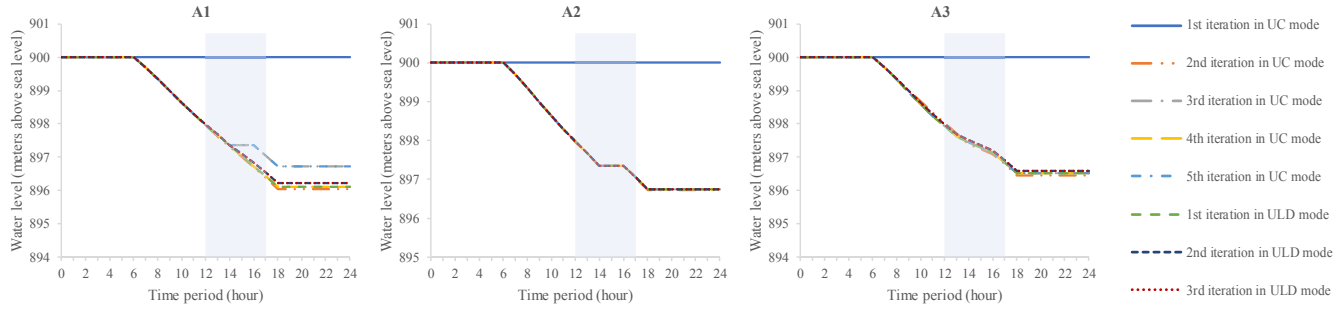

Fig. 12. The evolution of the water level of the reservoir before each iteration in A1, A2, and A3.

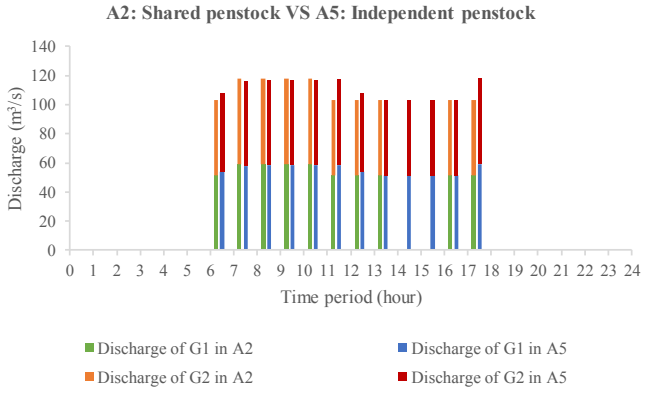

Fig. 13. The final water discharge in A2 and A5.

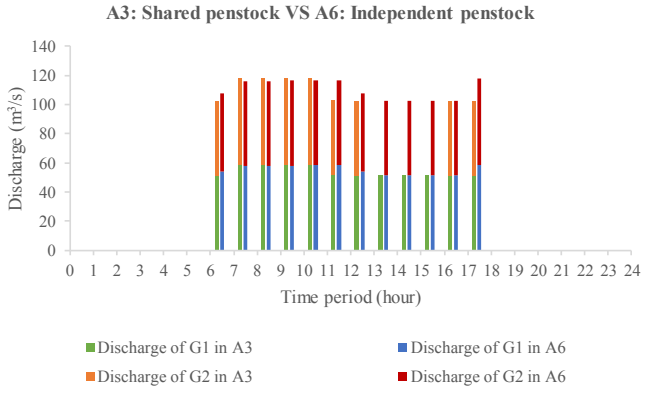

Fig. 14. The final water discharge in A3 and A6.

dotted line in Fig. 9). To obtain the maximum profit, the optimal result is to operate both units G1 and G2 at maximum. Since there is no inflow to the reservoir, the upstream reservoir will change from nearly full (32.77 Million m^3, 900 m) to almost empty (2.27 Million m^3, 864.8 m in A9; 2.81 Million m^3, 865.86 m in A10). Correspondingly, the net head at the operating point for G1 decreases from 214.16 m to 179.79 m in A9 (from 214.78 m to 182.14 m in A10), within the range of net head variation of the turbine as shown in Fig. 7 (or Fig. 8).

The turbine efficiency curves in A9 have the same minimum/maximum discharge limits for all effective heads (Fig. 7). We plot the I/O curves for G1 in every 12 h in the third iteration in the ULD mode in Fig. 15, visualizing the dynamic alteration of breakpoints of the I/O curves from the beginning to the end of the scheduling. With the decrease of the net head, the maximum production is declining from 115.6 MW to 95.95 MW while the maximum discharge is kept constantly at maximum (58.83 m^3/s). In the meantime, the minimum production is always 60 MW while the minimum discharge is rising from 30.78 m^3/s to 36.25 m^3/s. The optimal production and discharge of G1 during the entire scheduling horizon (red line in Fig. 15) vary with the maximum limit of the curve.

By contrast, in A10, the minimum/maximum discharge limits of the turbine efficiency curves are changeable with the net head (Fig. 8). Analogously, the transformation of the I/O curves for G1 in A10 is captured in Fig. 16. The maximum discharge first increases from 57.48 m^3/s to 58.81 m^3/s as the net head decreases but starts to decrease after the net head reaches 200 m. The head-dependent and nonlinear operating characteristics of the turbine efficiency curves are correctly reflected by the unit I/O curves and optimization result, indicating that the proposed method can appropriately represent the operational limits.

It is also worth emphasizing that most existing publication assumed that the breakpoints are predefined and fixed, but the method we propose does not require the breakpoints available in advance. Instead, the breakpoints are dynamically created per unit and period during the optimization and can be created as many as the users want by defining the number of segments $\bar{x}^{DOWN}$ and $\bar{x}^{UP}$. The whole set of unit I/O curves that cover all the possible net head is critical information for the hydropower producers in practice. This is the fundamental difference between our method and others. In other words, our method can be used as a premise for other methods that need the breakpoints ready before optimization.

Besides, in a hydro system with shared penstock, the I/O curve for one unit in one period is also influenced by the operating status of other units. For example, in A9, we now assume that G2 is under maintenance and only G1 is available. Then the I/O curves for G1 in the same hours totally change, as shown in Fig. 17. Since less water is charged from the reservoir, the decrease of the net head becomes much slower. Therefore, for a system with multi-level shared penstock configurations and multiple generating units, it is no longer suitable to use a family of unit I/O curves with fixed breakpoints to obtain a precise dispatch plan.

6.2. Test example B: a real hydro system

The real hydro system in Southern Norway is owned by Statkraft

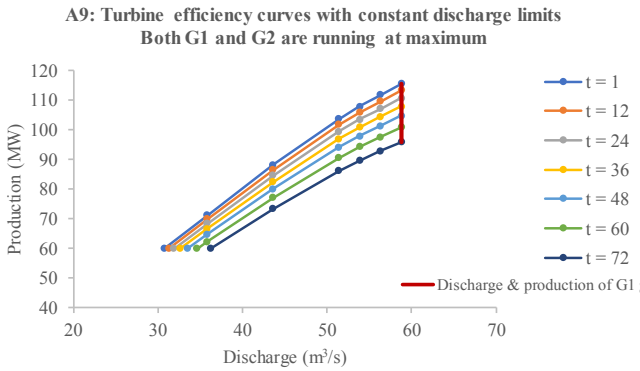

Fig. 15. The I/O curves for G1 in every 12 h in the third iteration in the ULD mode in A9 when both units are running at maximum.

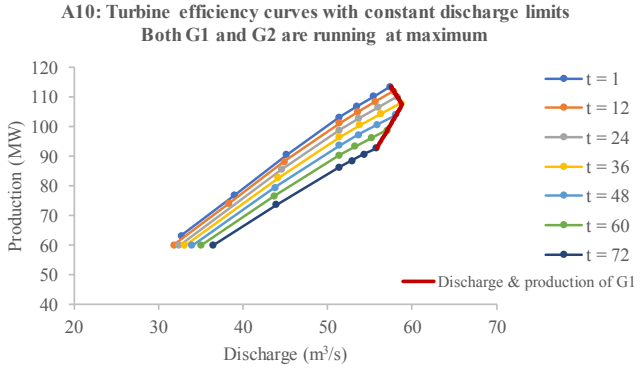

Fig. 16. The I/O curves for G1 in every 12 h in the fifth iteration in the ULD mode in A10 when both units are running at maximum.

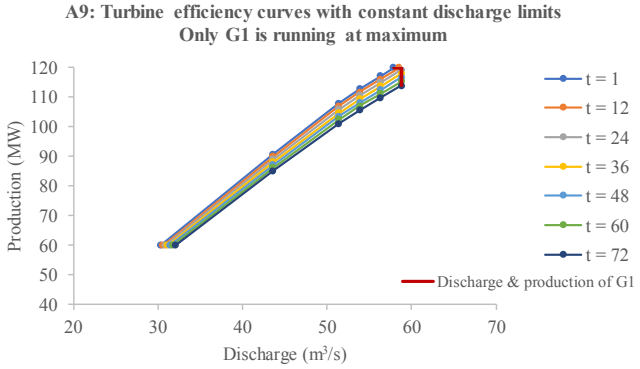

Fig. 17. The I/O curves for G1 in every 12 h in the third iteration in the ULD mode in A9 when only unit G1 is running at maximum.

Energi AS. The publicly available characteristic parameters of the hydropower plants and reservoirs are marked in Fig. 19[1]. This watercourse is modeled as 17 reservoirs (Reservoirs Kviteseidvatn and Flåvatn are merged as one reservoir), eight hydropower plants with 13 generating units (Plant Smørklepp I-II with a capacity of 0.7 MW is too small to be included), and two junctions. As illustrated in Fig. 18, multiple units in Plant Vinje (three different units) and Plant Tokke (four identical units) are fed by shared main tunnels and penstocks. Other plants have only one generating unit. There is tailrace loss in Plant Kjela and intake loss in Plant Tokke.

The scheduling purpose is to optimize energy delivery in the day-ahead market. A typical week in the spring is selected as the scheduling horizon, with inflow mainly from the melting snow. The time resolution is still one hour. In Fig. 20, the market price is illustrated. The water value for each reservoir is provided by a mid-term hydro scheduling model [44].

In this test example with real-world size, we create seven instances B1–B7 and conduct three comparisons, as shown in Table 6. In the first comparison, we investigate the influence of the three presented heuristics on calculational efficiency. We further analyze the impact of formulation accuracy on solution quality by testing different numbers of segments in the linearization of the HPF and power loss.

Table 7 first enumerates the relative profit changes between two consecutive iterations in both UC and ULD modes. For each iteration in the UC mode, the stopping criterion is that the relative MIP gap is no greater than 0.01%. The convergence measure is that the relative change in total profit between two consecutive iterations is less than 0.005%. Because of the mass inflow in the spring, the water values of most reservoirs are lower than the hourly market price in most periods. Reasonable unit start-up and shut-down costs are also introduced in the model. Therefore, no noticeable flip-flop takes place in those instances. As can be seen from Table 7, after four iterations in the UC mode and two iterations in the ULD mode, all the instances are convergent.

Table 7 then lists the number of binary/continuous variables, the number of constraints, relative MIP gap, time used in CPLEX, and the maximum unbalance between the total optimal power output of the units and the actual total power output based on the original nonlinear HPF, in the fourth iteration in the UC mode and the second iteration in the ULD mode, respectively. Note that given the presented method, only one binary variable is used per unit and period. The total number of binary variables in the UC mode is the same in all the instances (2184 = 13 units × 168 periods), no matter which heuristics are employed and how many segments are defined in the unit I/O curves. In addition, since only committed-to-run units will be included in the ULD mode, the optimization model becomes LP, and hence, there are no binary variables and MIP gap in the ULD mode. This is also the reason why the calculational time in the UC mode is overwhelmingly higher than that used in the ULD mode.

[1] There are two numeric mistakes on Fig. 19: Reservoir Vatjønn (938/935) should be Vatjønni (838/835), and Plant Byrte (430/2140) should be Byrte (24/135.3).

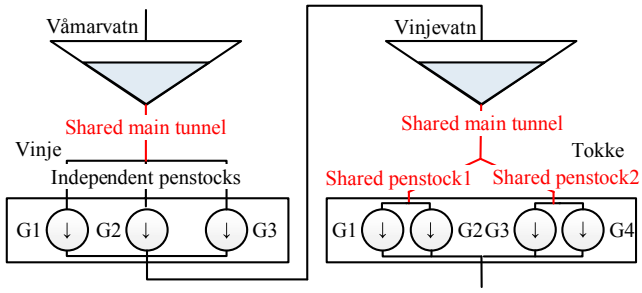

Fig. 18. Schematic diagram of Plants Vinje and Tokke.

Table 7 ends with a summary of the final result of each instance. The total time refers to the sum of the calculational time spent in the four iterations in the UC mode and the two iterations in the ULD mode. The total profit is the final solution obtained after all the iterations. For the sake of a clear comparison, the calculational time and profit changes are calculated relative to instance B3. The total profit varies subtly, while the calculational time differs significantly. Fig. 20 displays the hourly production of each plant in B3. The total production follows the trend of the market price. Other instances result in a similar production pattern.

6.2.1. *Comparison 5: the impact of the three heuristics on the calculational efficiency*

Comparison 5 is to study the influence of the proposed heuristics on the calculational efficiency. Instances B1–B3 are solved by heuristics H1–H3, respectively. As shown in Table 7, in the UC mode B1 and B2 have similar numbers of continuous variables and constraints, and the computational times for solving the two instances are alike. By contrast, because extra variables and constraints are introduced to handle the power loss in shared penstocks by H3, the calculational time in B3 obviously goes up. In the ULD mode, the number of variables and constraints is similar among all the three instances. This is due to the solution strategy, as discussed in Section 5, that only H1 is used in the ULD mode.

This comparison testifies that the choice of proper heuristic depends on the operating conditions. If the forecasted market price is undoubtedly higher or lower than the water value (e.g., in an extremely cold winter or spring flood), it is safe to adopt H1 to obtain a quick and reliable result. If the scheduling horizon is more than one week, and the hydropower producers participate in multiple markets (simultaneous optimization of both reserve capacity and energy delivery for individual units is very time-consuming, but this discussion is out of the scope of

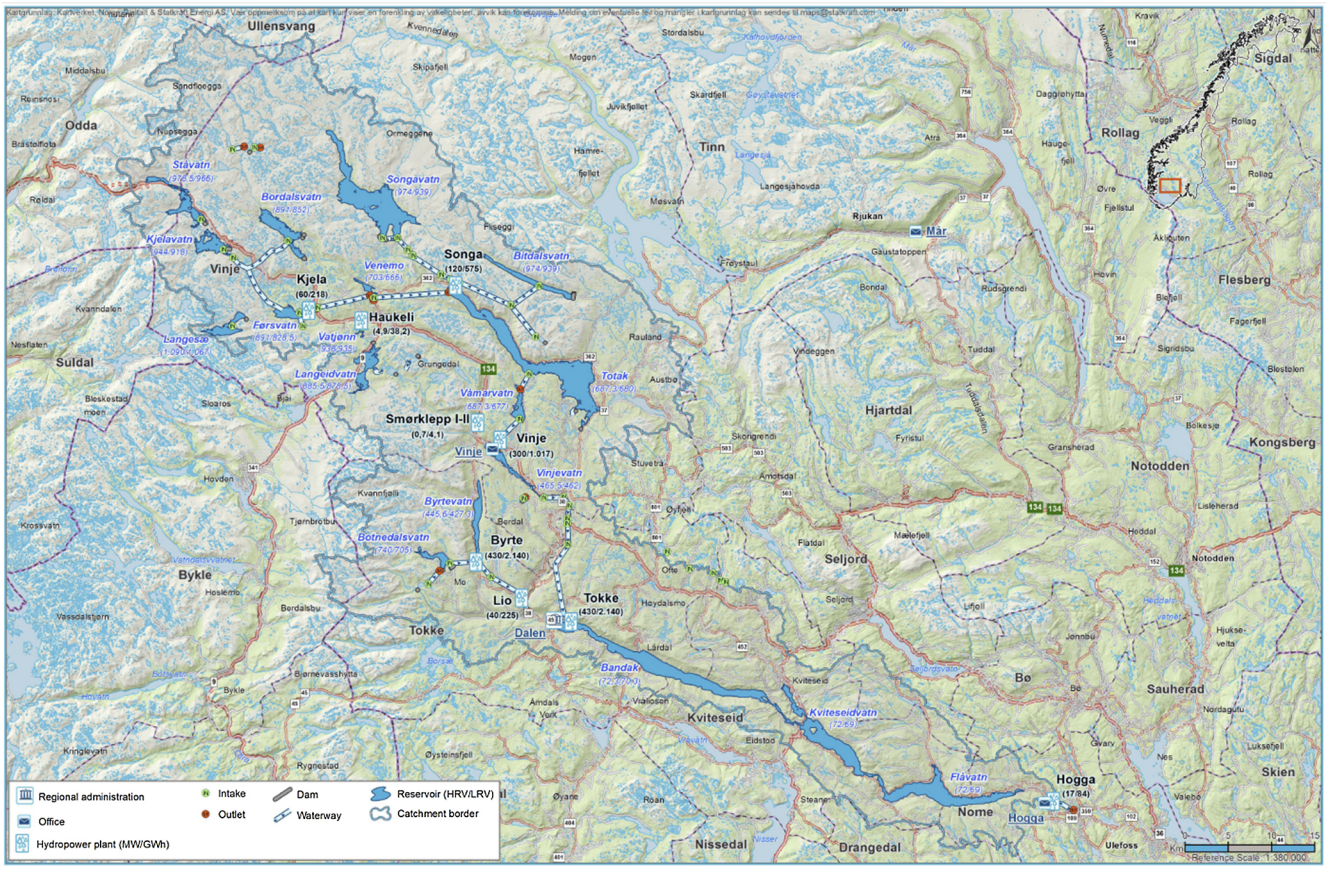

Fig. 19. Tokke catchment area (Source: Statkraft [45]).

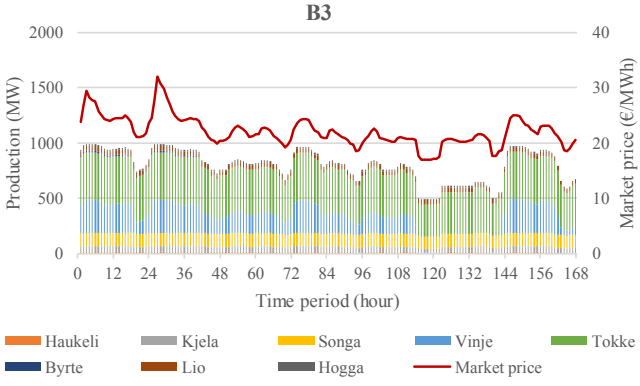

Fig. 20. Market price and production of each plant.

this paper), H2 is a candidate for acquiring an acceptable result. If the market price and the water value are close, and the scheduling is for the actual energy delivery for coming hours, H3 is recommended to guarantee the solution quality.

At last, we have to re-emphasize that these three heuristics are put forward for the existence of the shared penstock in the hydro system. If there are only independent penstocks, the three heuristics will lead to the same UC and dispatch decision, as discussed in *Comparison 2*.

6.2.2. *Comparison 6: the impact of the number of segments of the unit I/O curve on solution quality*

Comparison 6 is to check whether the increase of segments of the unit I/O curve will help to improve the solution quality. The total number of segments of the I/O curve per unit and period is 6 in B3, 20 in B4, and 40 in B5.

Table 6
Information for Instances B1–B7 under Comparisons 5–7.

Instance	Heuristic	No. of segments of unit I/O curve[a]	No. of segments of power loss curve[b]
Comparison 5: the impact of the three heuristics			
B1	H1	3 + 3	–
B2	H2	3 + 3	–
B3	H3	3 + 3	10
Comparison 6: the impact of no. of segments of unit I/O Curve			
B3	H3	3 + 3	10
B4	H3	10 + 10	10
B5	H3	20 + 20	10
Comparison 7: the impact of no. of segments of power loss curve			
B3	H3	3 + 3	10
B6	H3	3 + 3	20
B7	H3	3 + 3	10 + 2

Note:
[a] The first figure is the number of segments between the minimum water discharge and the best efficiency $\bar{x}^{DOWN}$. The second figure is the number of segments between the best efficiency and the maximum water discharge $\bar{x}^{UP}$.
[b] The figure is the number of segments of the power loss curve $\bar{y}$.

It can be seen from Table 7 that with the increase of the segments, the number of the continuous variables as well as the computational time are proportionally increasing. However, the reduction in the maximum unbalance is trivial, and the augmentation in the total profit is insignificant. The reason has been explained in [11]. Since the HPF is approximated by a concave piecewise linear curve, the quality of the approximation will rely on whether there is any non-concave region on the curve and where the optimal operating point is. If the HPF is mostly concave, the unbalance between the optimal power output obtained from the model and the actual power output computed from the HPF may become arbitrarily small by increasing the number of segments in

Table 7
Results for Instances B1–B7.

	Instance B1	B2	B3	B4	B5	B6	B7
Relative profit change between two consecutive iterations in the UC mode							
1st and 2nd iteration	−0.4732%	−0.0621%	−0.0283%	−0.0238%	−0.0288%	−0.0385%	−0.032%
2nd and 3rd iteration	−0.0083%	0.0456%	0.0320%	0.0294%	0.0280%	0.0405%	0.0305%
3rd and 4th iteration	0.0033%	−0.0018%	0.0003%	−0.0034%	0.0042%	0.0000%	−0.0005%
Relative profit change between two consecutive iterations in the ULD mode							
1st and 2nd iteration	0.0024%	−0.0001%	0.0004%	−0.0003%	0.0000%	0.0002%	0.0007%
4th iteration in the UC mode							
No. of binary variables	2,184	2,184	2,184	2,184	2,184	2,184	2,184
No. of continuous variables	48,027	47,809	56,933	77,531	100,102	63,687	51,495
No. of constraints	18,291	18,291	24,970	24,914	24,973	24,970	24,967
MIP gap	0.0069%	0.0073%	0.0095%	0.0093%	0.0100%	0.0069%	0.0018%
Time used in CPLEX (s)	17.72	15.94	42.37	50.91	95.57	39.78	30.73
Maximum unbalance (MW)	4.19	1.84	3.77	3.26	3.14	3.57	3.07
2nd iteration in the ULD mode							
No. of continuous variables	41,428	41,262	41,236	63,202	88,777	41,273	41,271
No. of constraints	13,117	13,050	13,027	13,033	12,992	13,038	13,024
Time used in CPLEX (s)	1.13	1.13	1.23	2.08	3.08	1.45	1.32
Maximum unbalance (MW)	0.31	0.31	0.32	0.30	0.30	0.33	0.31
Final result							
Total time used in CPLEX (s)	91.14	83.94	170.99	275.44	421.75	212.81	129.59
Relative time change to B3 (%)	−47%	−51%	–	61%	147%	24%	−24%
Total profit (€)	20,871,891	20,872,825	20,873,274	20,873,597	20,873,333	20,872,764	20,873,305
Relative profit change to B3 (%)	−0.0066%	−0.0022%	–	0.0015%	0.0003%	−0.0024%	0.0001%

the approximation. If the HPF is non-concave, the unbalance cannot be avoided, even if the segments grow in number. Take the non-concave region of G1 in Hour 7 as an example (Table 5). No matter how many breakpoints are added in the non-concave region ($28.12\,m^3/s$–$43.66\,m^3/s$), after convexification these breakpoints will be deleted from the I/O curve. If the optimal operating point ends up in this area, the unbalance hence occurs.

To sum up, simply raising the number of segments of the unit I/O curve leads to the increase in computational time but does not necessarily make the solution accuracy better. If the maximum unbalance is beyond the acceptable tolerance and heavily impairs the solution quality, other modeling approaches should be used to solve the problem.

6.2.3. Comparison 7: the impact of the number of segments of the power loss curve on solution quality

Comparison 7 is to examine the possibility of improving the solution quality by defining breakpoints of the power loss curve in various ways. In instance B3, the power loss curve is evenly divided into 10 segments, while in B6, the curve is partitioned into 20 segments. Different from B3 and B6, B7 takes advantage of the iterative solution strategy of SHOP. In the first iteration, the number of segments is 10. In the following iterations, the optimal water flow in the common penstock from the previous iteration is set as the unique breakpoint. Therefore, there are only two segments in the discretization of the power loss curve.

As shown in Table 7, the plain increase in the number of the segments of the power loss curve in B6 only brings about the growth of the calculational time, and even worse, the reduction of the total profit. By contrast, using the result from the previous iteration as the breakpoint in B7 reduces the number of continuous variables. It helps to notably lower the computational time without scaling down the solution quality.

It is worth mentioning that the use of the previous optimal result as the sole breakpoint is acceptable only if the operating point of the hydro system is stable. In B7, it works well after the first iteration. However, due to the hydraulic complexity of the system, how many iterations are needed to find a stable UC is uncertain. If the previous result as the only breakpoint is adopted too early, there would be the risk of ending up in a suboptimal solution.

7. Conclusion

This paper presents a MILP model that aims at solving the unit-based STHS problem for daily operation. Special attention is given to the representation of details of the HPF, including all relevant factors that affect the power output. Thus, by considering the time-varying head effect, intake loss, penstock loss, tailrace loss, and head-dependent turbine efficiency simultaneously, we can obtain an accurate solution for the problem, which is significant for the pwoer systems with high participation of hydropower generation.

A new method is presented to convert the nonlinear and non-convex HPF to the convex piecewise linear approximation with dynamically specified breakpoints. Three heuristics are explored to incorporate the nonlinear power loss in shared penstocks in the STHS problem. The developed method and heuristics have been implemented in an operational STHS tool used by many large hydropower producers in Scandinavia.

Numerical results indicate that the proposed method for approximating the HPF can precisely reflect the head-dependent operating limits of the unit. Different comparisons show that the effect of power loss in shared penstocks cannot be ignored. The appropriate representation of the power loss is crucial for obtaining the optimal UC decision. By heuristic H1, when the forecasted market price for electricity is close to the marginal water value of the reservoir at the end of the scheduling horizon, the power production is likely to oscillate between iterations. H2 can avoid this problem but always suggests that the units operate in the same pattern. H3 gives a better optimization result but increases the computational time by introducing more variables and constraints. None of the three heuristics is perfect, but they can be flexibly applied to cover the needs of the producers in the real-world operation. If a quick solution time has the priority, H1 or H2 is recommended. If precision matters, H3 should be chosen.

Future improvements in modeling techniques and research interests will focus on these aspects: (1) Instead of including the production bounds and interpolating the final discharge limits after the unit I/O curve is built (*Step 8* in Section 4), all the operational constraints can be simultaneously taken into consideration in *Step 2*. This will give a more accurate result when the unit must operate at limits, e.g., run at some low production level to keep the outflow constant; (2) The convexification of the non-concave I/O curve may result in the deviations

between the power output from the optimization model and the power output directly calculated from the nonlinear HPF. Actually, an increase in the number of breakpoints in the discretization does not necessarily lead to better representation, since all the points in the non-concave part of the I/O curve will be eliminated. Therefore, a new solution methodology is needed to find the balance between the accurate representation of the non-convex part of the curve and low calculational burden; (3) It is noticed that the relationship between the market price and the water value of the reservoir at the end of the scheduling horizon has a significant impact on the production schedules. How to define the energy conversion factor that converts the end value of the reservoir from water to energy, which is currently taken as a given parameter, is hence crucial; (4) Intake and tailrace losses are included in the calculation of the gross head by using the previous optimal discharge results. It would cause the same oscillation problem as H1 in some situations. An approach for incorporating the intake and tailrace losses in the current iteration should be developed; (5) As shown in *Comparison 4*, the proposed method can create a family of unit I/O curves spanning the possible net head area, considering the operating status of other units in the same plant. It would be meaningful to determine in which situation it is more efficient to create the breakpoints in advance than to dynamically create breakpoints during optimization; (6) last but not least, at the moment only one heuristic can be chosen in the UC mode to handle the power loss in the shared penstocks. The selected heuristic is valid for the entire scheduling periods. It would be interesting to see whether the combination of the heuristics would result in higher profit. However, the right combinations of heuristics for the optimization model are hidden behind thousands of the complex constraints and millions of the coupling variables. Therefore, big data analysis can be are applied to accommodate all the available options.

Declaration of Competing Interest

The authors declared that there is no conflict of interest.

Acknowledgements

The authors would like to acknowledge the contributions of other developers for the testing and calibration of SHOP. The authors wish to thank Dr. T. J. Larsen and Mr. F. Kristiansen at Statkraft Energi AS for providing the test data and validating the results. The authors are also indebted to the anonymous referees for many valuable comments that helped to restructure this paper and made it more readable and accessible to both theoreticians and practitioners.

References

[1] Piekutowski MR, Litwinowicz T, Frowd RJ. Optimal short-term scheduling for a large-scale cascaded hydro system. IEEE Trans Power Syst 1994;9:805–11. https://doi.org/10.1109/59.317636.
[2] Chang GW, Aganagic M, Waight JG, Medina J, Burton T, Reeves S, et al. Experiences with mixed integer linear programming based approaches on short-term hydro scheduling. IEEE Trans Power Syst 2001;16:743–9. https://doi.org/10.1109/59.962421.
[3] Garcia-Gonzalez J, Castro GA. Short-term hydro scheduling with cascaded and head-dependent reservoirs based on mixed-integer linear programming. 2001 IEEE Power Tech Conference, Porto, PORTUGAL 2001. https://doi.org/10.1109/PTC.2001.964906.
[4] Borghetti A, D'Ambrosio C, Lodi A, Martello S. An MILP approach for short-term hydro scheduling and unit commitment with head-dependent reservoir. IEEE Trans Power Syst 2008;23:1115–24. https://doi.org/10.1109/tpwrs.2008.926704.
[5] Garcia-Gonzalez J, Parrilla E, Mateo A. Risk-averse profit-based optimal scheduling of a hydro-chain in the day-ahead electricity market. Eur J Oper Res 2007;181:1354–69. https://doi.org/10.1016/j.ejor.2005.11.047.
[6] Tong B, Zhai QZ, Guan XH. An MILP based formulation for short-term hydro generation scheduling with analysis of the linearization effects on solution feasibility. IEEE Trans Power Syst 2013;28:3588–99. https://doi.org/10.1109/tpwrs.2013.2274286.
[7] Cheng CT, Wang JY, Wu XY. Hydro unit commitment with a head-sensitive reservoir and multiple vibration zones using MILP. IEEE Trans Power Syst 2016;31:4842–52. https://doi.org/10.1109/tpwrs.2016.2522469.
[8] Taktak R, D'Ambrosio C. An overview on mathematical programming approaches for the deterministic unit commitment problem in hydro valleys. Energy Syst 2017;8:57–79. https://doi.org/10.1007/s12667-015-0189-x.
[9] Li X, Li TJ, Wei JH, Wang GQ, Yeh WWG. Hydro unit commitment via mixed integer linear programming: a case study of the three gorges project, China. IEEE Trans Power Syst 2014;29:1232–41. https://doi.org/10.1109/tpwrs.2013.2288933.
[10] Hamann A, Hug G, Rosinski S. Real-time optimization of the Mid-Columbia hydropower system. IEEE Trans Power Syst 2017;32:157–65. https://doi.org/10.1109/tpwrs.2016.2550490.
[11] Diniz AL, Maceira MEP. A four-dimensional model of hydro generation for the short-term hydrothermal dispatch problem considering head and spillage effects. IEEE Trans Power Syst 2008;23:1298–308. https://doi.org/10.1109/tpwrs.2008.922253.
[12] Seguin S, Cote P, Audet C. Self-scheduling short-term unit commitment and loading problem. IEEE Trans Power Syst 2016;31:133–42. https://doi.org/10.1109/tpwrs.2014.2383911.
[13] Guedes LSM, Maia PD, Lisboa AC, Gomes Vieira DA, Saldanha RR. A unit commitment algorithm and a compact MILP model for short-term hydro-power generation scheduling. IEEE Trans Power Syst 2017;32:3381–90. https://doi.org/10.1109/tpwrs.2016.2641390.
[14] Santos TN, Diniz AL. A comparison of static and dynamic models for hydro production in generation scheduling problems. 2010 IEEE Power and Energy Society General Meeting, Providence, RI, USA 2010. https://doi.org/10.1109/PES.2010.5589895.
[15] Arce A, Ohishi T, Soares S. Optimal dispatch of generating units of the Itaipu hydroelectric plant. IEEE Trans Power Syst 2002;17:154–8. https://doi.org/10.1109/59.982207.
[16] Finardi EC, Scuzziato MR. Hydro unit commitment and loading problem for day-ahead operation planning problem. Int J Electr Power Energy Syst 2013;44:7–16. https://doi.org/10.1016/j.ijepes.2012.07.023.
[17] Lu P, Zhou JZ, Wang C, Qiao Q, Mo L. Short-term hydro generation scheduling of Xiluodu and Xiangjiaba cascade hydropower stations using improved binary-real coded bee colony optimization algorithm. Energy Conv Manag 2015;91:19–31. https://doi.org/10.1016/j.enconman.2014.11.036.
[18] Santo TD, Costa AS. Hydroelectric unit commitment for power plants composed of distinct groups of generating units. Electr Power Syst Res 2016;137:16–25. https://doi.org/10.1016/j.epsr.2016.03.037.
[19] Soares S, Salmazo CT. Minimum loss predispatch model for hydroelectric power systems. IEEE Trans Power Syst 1997;12:1220–7. https://doi.org/10.1109/59.630464.
[20] Finardi EC, da Silva EL. Unit commitment of single hydroelectric plant. Electr Power Syst Res 2005;75:116–23. https://doi.org/10.1016/j.epsr.2005.01.008.
[21] Finardi EC, da Silva EL. Solving the hydro unit commitment problem via dual decomposition and sequential quadratic programming. IEEE Trans Power Syst 2006;21:835–44. https://doi.org/10.1109/tpwrs.2006.873121.
[22] Fosso OB, Gjelsvik A, Haugstad A, Mo B. Wangensteen I. Generation scheduling in a deregulated system. The Norwegian case. IEEE Trans Power Syst 1999;14:75–80. https://doi.org/10.1109/59.744487.
[23] Cordova MM, Finardi EC, Ribas FAC, de Matos VL, Scuzziato MR. Performance evaluation and energy production optimization in the real-time operation of hydropower plants. Electr Power Syst Res 2014;116:201–7. https://doi.org/10.1016/j.epsr.2014.06.012.
[24] Kong J, Skjelbred HI, Abgottspon H. Short-term hydro scheduling of a variable speed pumped storage hydropower plant considering head loss in a shared penstock. 2018 29th IAHR Symposium on Hydraulic Machinery and Systems, Kyoto, JAPAN 2018. https://doi.org/10.1088/1755-1315/240/4/042011.
[25] Xu BB, Wang FF, Chen DY, Zhang H. Hamiltonian modeling of multi-hydro-turbine governing systems with sharing common penstock and dynamic analyses under shock load 2016;108:478–87. https://doi.org/10.1016/j.enconman.2015.11.032.
[26] Breton M, Hachem S, Hammadia A. Accounting for losses in the optimization of production of hydroplants. IEEE Trans Energy Convers 2004;19:346–51. https://doi.org/10.1109/tec.2004.827043.
[27] Bortoni EC, Bastos GS, Abreu TM, Kawkabani B. Online optimal power distribution between units of a hydro power plant. Renew Energ 2015;75:30–6. https://doi.org/10.1016/j.renene.2014.09.009.
[28] Liao SL, Zhao HY, Li G, Liu BX. Short-term load dispatching method for a diversion hydropower plant with multiple turbines in one tunnel using a two-stage model 2019;12. https://doi.org/10.3390/en12081476.
[29] Lima RM, Marcovecchio MG, Novais AQ, Grossmann IE. On the computational studies of deterministic global optimization of head dependent short-term hydro scheduling. IEEE Trans Power Syst 2013;28:4336–47. https://doi.org/10.1109/tpwrs.2013.2274559.
[30] Fosso OB, Belsnes MM. Short-term hydro scheduling in a liberalized power system. 2004 international conference on power system technology (POWERCON), Singapore, Singapore 2004. p. 1321–6. https://doi.org/10.1109/ICPST.2004.1460206.
[31] Alvarez M, Ronnberg SK, Bermudez J, Zhong J, Bollen MHJ. Reservoir-type hydropower equivalent model based on a future cost piecewise approximation 2018;155:184–95. https://doi.org/10.1016/j.epsr.2017.09.028.
[32] Skjelbred HI, Kong J. Operational hydropower simulation in cascaded river systems for intraday re-planning. 2018 20th Power Systems Computation Conference (PSCC), Dublin, IRELAND 2018. https://doi.org/10.23919/PSCC.2018.8442510.
[33] Shawwash ZK, Siu TK, Russell SOD. The B.C. Hydro short term hydro scheduling optimization model. IEEE Trans Power Syst 2000;15:1125–31. https://doi.org/10.1109/59.871743.
[34] Perez-Diaz JI, Wilhelmi JR, Arevalo LA. Optimal short-term operation schedule of a

hydropower plant in a competitive electricity market. Energy Conv Manag 2010;51:2955–66. https://doi.org/10.1016/j.enconman.2010.06.038.
[35] De Ladurantaye D, Gendreau M, Potvin JY. Optimizing profits from hydroelectricity production. Comput Oper Res 2009;36:499–529. https://doi.org/10.1016/j.cor.2007.10.012.
[36] Sousa T, Jardini JA, de Lima RA. In site hydroelectric power plant unit efficiency measurement. 2010 IEEE PES transmission and distribution conference and exposition, New Orleans, LA, USA 2010. https://doi.org/10.1109/TDC.2010.5484627.
[37] Skjelbred HI, Kong J. A comparison of linear interpolation and spline interpolation for turbine efficiency curves in short-term hydropower scheduling problems. 2018 29th IAHR symposium on hydraulic machinery and systems, Kyoto, JAPAN 2018. https://doi.org/10.1088/1755-1315/240/8/082002.
[38] Hidalgo IG, Fontane DG, Lopes JEG, Andrade JGP, de Angelis AF. Efficiency curves for hydroelectric generating units. J Water Resour Plan Manage-ASCE. 2014;140:86–91. https://doi.org/10.1061/(asce)wr.1943-5452.0000258.
[39] Belsnes MM, Wolfgang O, Follestad T, Aasgård EK. Applying successive linear programming for stochastic short-term hydropower optimization. Electr Pow Syst Res. 2016;130:167–80. https://doi.org/10.1016/j.epsr.2015.08.020.
[40] Skjelbred HI, Kong J, Larsen TJ, Kristiansen F. Operational use of marginal cost curves for hydropower plants as decision support in real-time balancing markets. 2017 14th international conference on the european energy market (EEM), Dresden, Germany 2017. https://doi.org/10.1109/eem.2017.7981875.
[41] Kong J, Skjelbred HI. Operational hydropower scheduling with post-spot distribution of reserve obligations. 2017 14th international conference on the european energy market (EEM), Dresden, Germany 2017. https://doi.org/10.1109/eem.2017.7981874.
[42] Marchand A, Gendreau M, Blais M, Emiel G. Fast near-optimal heuristic for the short-term hydro-generation planning problem. IEEE Trans Power Syst 2018;33:227–35. https://doi.org/10.1109/tpwrs.2017.2696438.
[43] NordPool. https://www.nordpoolgroup.com/. [accessed 2019-07-08].
[44] Mo B, Gjelsvik A, Grundt A. Integrated risk management of hydro power scheduling and contract management. IEEE Trans Power Syst 2001;16:216–21. https://doi.org/10.1109/59.918289.
[45] Statkraft. https://www.statkraft.com/energy-sources/hydropower/maps-over-catchment-areas-in-norway/. [accessed 2019-07-01].